

# Mesoscale Field Theory for Quasicrystals

Marcello De Donno,<sup>1</sup> Luiza Angheluta,<sup>2</sup> Ken R. Elder,<sup>3</sup> and Marco Salvalaglio<sup>1,4,\*</sup>

<sup>1</sup>*Institute of Scientific Computing, TU Dresden, 01062 Dresden, Germany*

<sup>2</sup>*Njord Centre, Department of Physics, University of Oslo, 0371 Oslo, Norway*

<sup>3</sup>*Department of Physics, Oakland University, Rochester, Michigan 48309, USA*

<sup>4</sup>*Dresden Center for Computational Materials Science (DCMS), TU Dresden, 01062 Dresden, Germany*

We present a mesoscale field theory unifying the modeling of growth, elasticity, and dislocations in quasicrystals. The theory is based on the amplitudes entering their density-wave representation. We introduce a free energy functional for complex amplitudes and assume non-conserved dissipative dynamics to describe their evolution. Elasticity, including phononic and phasonic deformation, defect nucleation and motion, emerges self-consistently by prescribing only the symmetry of quasicrystals. Predictions on the formation of semi-coherent interfaces and dislocation kinematics are given.

Quasicrystals (QCs) are aperiodic yet ordered arrangements that lack translational symmetry but still possess rotational symmetry. They exhibit distinctive, discrete diffraction patterns, which have been instrumental to their discovery [1, 2] and detection in both synthetic and natural materials [3–6]. QCs exhibit exotic features such as low friction and thermal conductivity, nonstick surface properties, and peculiar electronic properties [7, 8]. Importantly, quasicrystalline order can be found in various systems, spanning from solid-state materials to soft matter [9–15]. Moreover, QCs are intimately related to mathematical tiling concepts explored well before their discovery in actual materials [16, 17] and emerge in more exotic systems such as vibrating (macroscopic) granular materials [18] and quantum phase transitions [19].

QCs can be constructed via different procedures from a periodic hyperlattice [20, 21]. Via the *strip-projection* method, for instance, one considers the hyperlattice points within two parallel (flat) hypersurfaces (a hyper-strip) oriented with an irrational slope w.r.t. the hyperlattice orientations. The aperiodic structure is obtained by projecting the lattice positions on one of these hypersurfaces. A classic example is the 1D aperiodic arrangement corresponding to the Fibonacci sequence constructed from a 2D square lattice with this method [22]. Similarly, a 2D ten-fold QC [23] or the iconic 3D icosahedral QC [1] can be constructed from periodic lattices in 4D and 6D hyperspaces, respectively.

A natural description leveraging *discrete diffraction diagrams* [24] is obtained via a smooth, dimensionless density field  $\psi \equiv \psi(\mathbf{r})$  expanded in *density-waves* [20, 25]

$$\psi = \psi_0 + \sum_{n=1}^N \eta_n e^{i\mathbf{G}_n \cdot \mathbf{r}} + \text{c.c.}, \quad (1)$$

with  $i$  the imaginary unit, c.c. is the complex conjugate and  $\{\mathbf{G}_n\}$  the *discrete* set of reciprocal-space vectors, at which diffraction peaks are expected [26]. The complex amplitude functions,  $\eta_n = \phi_n e^{i\theta_n}$  are slowly varying (hydrodynamic) fields, and  $\psi_0$  is the average density, which is here set to zero for simplicity. The amplitudes encode lattice deformations through their phases  $\theta_n$ .

The density-wave representation (1) links directly to Landau's theories of phase transitions through free energy functionals  $F[\psi]$ . Free energies for bulk QCs have been discussed in seminal works [27, 28]. Approaches like the Swift-Hohenberg model [29, 30], the phase field crystal model (PFC) [31], as well as the classical density functional theory [32, 33], are based on free energies for smooth density fields where deformations and interfaces can also be described. Though primarily applied to ordered and periodic systems, they have yielded remarkable results for QCs too [34–39]. These methods, however, focus on microscopic length scales, preventing the description of large-scale systems and mechanical properties approaching continuum limits. In this Letter, building on coarse-graining concepts introduced for microscopic densities in crystalline systems [40–42], we introduce and demonstrate a self-consistent mesoscale field theory for QCs that closes this gap handling growth, elasticity, and dislocations by focusing on the complex amplitudes  $\{\eta_n\}$ .

We consider a dimensionless free energy functional of the form,

$$F_\eta = \int_{\Omega} \left\{ \sum_{n=1}^N (A |\mathcal{G}_n \eta_n|^2) + \sum_{k=2}^P (B_k \zeta_k) \right\} d\mathbf{r}, \quad (2)$$

with dissipative dynamics consistent with prior work [40, 42], i.e.,

$$\partial_t \eta_n = -\frac{\delta F_\eta}{\delta \eta_n^*} = A \mathcal{G}_n^2 \eta_n + \sum_{k=2}^P B_k \partial_{\eta_n^*} \zeta_k, \quad (3)$$

$A$  and  $B_k$  parameters,  $\mathcal{G}_n = \nabla^2 + 2i\mathbf{G}_n \cdot \nabla$ , and  $\zeta_k$  a polynomial of order  $k$  in the amplitudes and their complex conjugates such that the sum of the corresponding wave vector vanishes, a condition called *resonance condition* [42]. For instance,  $\zeta_2 = \sum_{p,q} \eta_p \eta_q \delta_{\mathbf{0}, \mathbf{G}_p + \mathbf{G}_q} = 2 \sum_{n=1}^N |\eta_n|^2 = \Phi$ , with  $p, q$  ranging between  $-N$  and  $N$  excluding 0,  $\eta_{-n} = \eta_n^*$ , and  $\mathbf{G}_{-n} = -\mathbf{G}_n$ .  $\Phi$  also plays the role of an order parameter for the (quasi-) crystalline order, as shown below. For  $P = 4$ , Eq. (2) can be derived from the Swift-Hohenberg free energy functional [29–31] upon coarse-graining via integration over

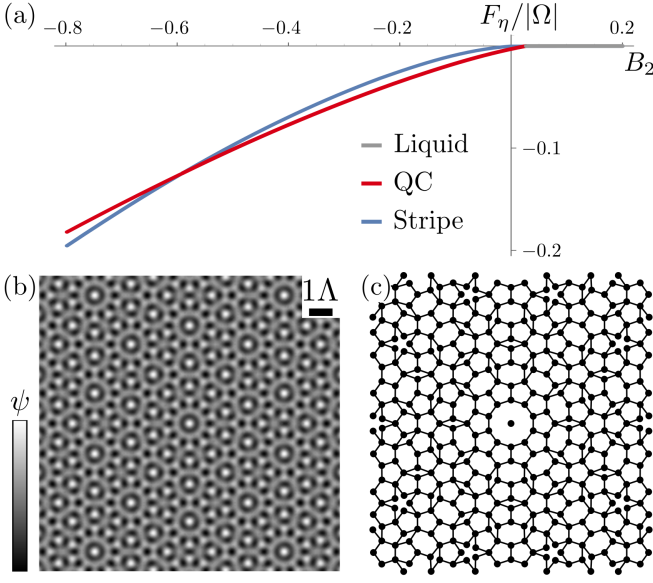


FIG. 1. *Decagonal QC phase as minimizer of the free energy* (2). (a) Free energy density for different phases varying  $B_2$  with  $B_4 = 0$ ,  $B_5 = -100$ ,  $B_6 = 0.1$  (independent of  $A$ ). (b)  $\psi$  reconstructed via Eq. (1) for  $B_2 = 0.02$ .  $\Lambda = 12.5932$ . (c) Tiling reconstructed from  $\psi$  (see also SM [45]).

the unit cell (UC) to average out microscopic oscillations [40, 42]. While a UC cannot be defined for QCs, quasi-UC descriptions [43] featuring overlapping local motifs were proposed and verified experimentally [44]. Accordingly, we found that averaging  $\psi$  for QCs results in a uniform field above a characteristic average width  $\Lambda$ , justifying the approach; see also the Supplemental Material (SM) [45]. The first term in Eq. (2) follows from the excess energy term  $\psi(q_0^2 + \nabla^2)^2 \psi$  [31] with  $q_0 = 1$  setting the characteristic wave number. We focus here on QCs which may be characterized by  $\{\mathbf{G}_n\}$  with the same length, like decagonal and icosahedral QCs, and  $|\mathbf{G}_n| = q_0 = 1$ . The second term in Eq. (2) encodes the local free-energy energy density and follows from powers of the microscopic density. The coefficients  $B_k$  in Eq. (2) can be chosen to minimize a specific crystal symmetry. For typical QCs, this is achieved for  $P > 4$ , thus requiring formulations beyond those typically used for crystals [42]. In all cases,  $P$  must be even to avoid divergent solutions for  $\eta_n$ .

As prominent examples, decagonal and icosahedral QCs are well described by  $\mathbf{G}_n^D = [\cos(2\pi n/5), \sin(2\pi n/5)]$  for  $1 \leq n \leq 5$  [23], and  $\mathbf{G}_n^I = (1/\sqrt{5})[2 \cos(2\pi n/5), 2 \sin(2\pi n/5), 1]$  for  $1 \leq n \leq 5$  plus  $\mathbf{G}_6^I = [0, 0, 1]$  [1], respectively. The first resonant terms are  $\zeta_5 = \prod_{j=1}^5 \eta_j + \text{c.c.}$ , so we need to consider the next even term,  $P = 6$ . Full expressions of the free energies are reported in the SM [45]. Hereafter we focus on decagonal QCs. Fig. 1a shows that a QC phase minimizes the free energy for some parameters. We vary  $B_2$ , corresponding to a phenomenological temperature

parameter in analogy with classical PFC models [31]. Consistently, for large  $B_2$ , disordered/liquid phases are favored, while first QCs and then stripe phases minimize the free energy when decreasing  $B_2$ . Fig. 1b shows the reconstructed density via Eq. (1) for the QC phase, while Fig. 1c illustrates a tiling reconstructed from the density peaks. By considering  $\psi_0 \neq 0$  and spatially dependent, the theory can be straightforwardly extended to admit phase coexistence [42, 46], whose discussion is however beyond the scope of the present work.

The free energy, Eq. (2), and the corresponding dynamics, Eq. (3), enable the characterization of out-of-equilibrium settings, their evolution, and the deformation of QCs. Moreover, deformations and defects in QCs can be fully characterized via the phase of the complex amplitudes  $\{\eta_n\}$ . Consider a periodic hyperlattice  $\mathcal{L}$  in a hyperspace with coordinates  $\tilde{\mathbf{r}} = \mathbf{r}^\parallel \oplus \mathbf{r}^\perp$ , with  $\mathbf{r}^\parallel = \mathbf{r}$  the coordinates the so-called *parallel* space ( $\Omega^\parallel = \Omega$ ), the physical space of definition of the quasicrystal, and  $\mathbf{r}^\perp$  the coordinates of the so-called *perpendicular* space ( $\Omega^\perp$ ) [22], required to define  $\mathcal{L}$  in addition to  $\Omega^\parallel$ . Deformation of  $\mathcal{L}$  can be generally described by the displacement field  $\tilde{\mathbf{U}} = \mathbf{u} \oplus \mathbf{w}$  with  $\mathbf{u}$  and  $\mathbf{w}$  being the displacements in  $\Omega^\parallel$  and  $\Omega^\perp$ , called *phonons* and *phasons*, respectively. From the deformation of the periodic density  $\tilde{\psi}(\tilde{\mathbf{r}} - \tilde{\mathbf{U}})$  of  $\mathcal{L}$ , the QC density  $\psi = \tilde{\psi}(\tilde{\mathbf{r}})|_{\mathbf{r}^\perp=0}$  results

$$\psi = \sum_{n=1}^N \underbrace{\phi_n}_{\eta_n} e^{-i\theta_n} e^{i\mathbf{G}_n \cdot \mathbf{r}} + \text{c.c.}, \quad (4)$$

$$\theta_n = \arg(\eta_n) = \mathbf{G}_n^\parallel \cdot \mathbf{u} + \mathbf{G}_n^\perp \cdot \mathbf{w},$$

with  $\mathbf{G}_n^\parallel = \mathbf{G}_n$  and  $\mathbf{G}_n^\perp$  can be constructed from  $\mathbf{G}_n^\parallel$  according to the QC rotational symmetry. Following Refs. [20, 25] for the decagonal QC we set  $\mathbf{G}_n^\perp = a\mathbf{G}_{(3n \bmod 5)}^\parallel$  with  $a = (1 + \sqrt{5})/2$  [45]. Note that the phase  $\theta_n$  depends on both deformations  $\mathbf{u}$  and  $\mathbf{w}$ . Dislocations in QCs inherently induce both phononic and phasonic deformations [20, 25] as they correspond to topological defects in the phase  $\theta_n$  with the topological charge given by

$$\oint d\theta_n = -2\pi s_n = -(\mathbf{G}_n^\parallel \cdot \mathbf{b}^\parallel + \mathbf{G}_n^\perp \cdot \mathbf{b}^\perp), \quad (5)$$

$s_n$  the winding (integer) number,  $\mathbf{b}^\parallel = \oint d\mathbf{u}$  and  $\mathbf{b}^\perp = \oint d\mathbf{w}$  Burgers vectors in  $\Omega^\parallel$  and  $\Omega^\perp$ , respectively.

An out-of-equilibrium system is illustrated in Fig. 2a by a numerical simulation of Eq. (3) using a Fourier pseudo-spectral method for spatial discretization [42, 45], exploited for all the following numerical examples. Slightly misoriented quasicrystalline seeds (i.e., rotated by some angle  $\alpha$ ) are considered. Using parameters that favor a QC phase, the initial seeds grow and eventually merge with the formation of topological defects, as indicated by localized regions where  $\Phi$  decreases, pointing

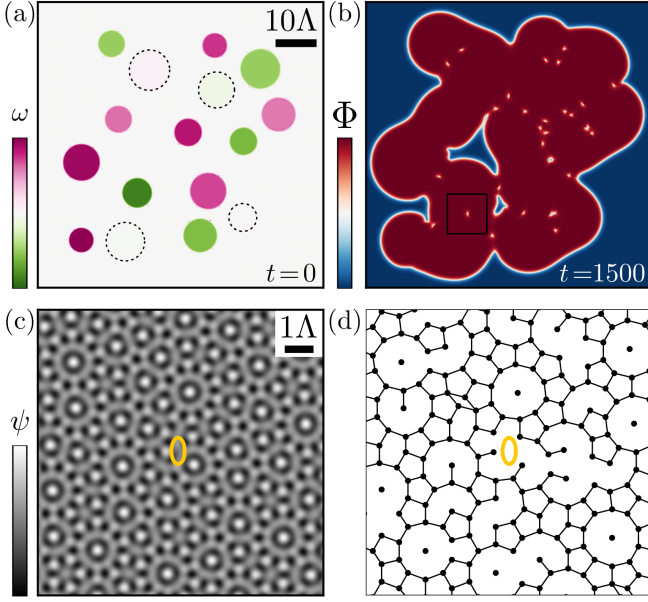


FIG. 2. *Growth of QCs seeds and defect nucleation.* (a) Rotation field  $\omega$  at  $t = 0$  initialized via amplitudes  $\eta_n = \phi_n \exp(i(M(\alpha)\mathbf{G}_n^{\parallel} - \mathbf{G}_n^{\parallel}) \cdot \mathbf{r})$  with  $M(\alpha)$  the standard rotation matrix [42] and  $|\alpha| \leq 5^\circ$ . Grains with a small rotation are illustrated by dashed lines. (b) Representative stage of growth, illustrated by  $\Phi$ . (c) and (d)  $\psi$  and tiling in the region marked by the black square in panel (b) with a (yellow) isoline at  $\Phi/\Phi_{\max} = 0.7$  showing the defect location. Parameters as in Fig. 1b with  $A = 1$ .

to a loss of quasicrystalline order. Figures 2c and 2d show the reconstructed density  $\psi$  and the tiling around a defect, deviating from the bulk, unperturbed phase (see Fig. 1). The proposed framework thus allows for the description of not only bulk systems but also complex phases in out-of-equilibrium settings, including interfaces, deformations, and defects.

A self-consistent elasticity theory for QCs follows upon deformation of  $\psi$ . The elastic energy, including all terms depending on deformation gradients, is  $\mathcal{E} = \int e(\nabla \mathbf{u}, \nabla \mathbf{w}) d\mathbf{r} = \int \{A \sum_{n=1}^N |\mathcal{G}_n \eta_n|^2\} d\mathbf{r}$ . The stress fields can be computed from  $\{\eta_n\}$  by taking the variational of this strain energy w.r.t independent variations of displacements,  $\delta \mathcal{E} = \int (\sigma_{ij}^{\parallel} \partial_j \delta u_i + \sigma_{ij}^{\perp} \partial_j \delta w_i) d\mathbf{r}$ , where summation over repeated indices is implied. Here,

$$\begin{aligned} \sigma_{ij}^S &= 4A \sum_{n=1}^N G_{n,i}^S \text{Im} \left[ (\mathcal{G}_n^* \eta_n^*) ((\partial_j + iG_{n,j}^{\parallel}) \eta_n) \right] \\ &\approx 8\phi_0^2 A \sum_{n=1}^N G_{n,i}^S G_{n,j}^{\parallel} G_{n,k}^{\parallel} \partial_k \theta_n, \end{aligned} \quad (6)$$

in  $\Omega^S$  with  $S = (\parallel, \perp)$  (see all derivation steps in the SM [45]). The second expression is obtained by retaining only the first derivatives of the phases and gives rise to the constitutive strain-stress relations of linear elastic-

ity. For small distortions, the elastic energy density reduces to the quadratic form  $2e(\nabla \mathbf{u}, \nabla \mathbf{w}) = C_{ijkl} \varepsilon_{ij} \varepsilon_{kl} + K_{ijkl} \partial_j w_i \partial_l w_k + R_{ijkl} \varepsilon_{ij} \partial_l w_k + R'_{ijkl} \partial_j w_i \varepsilon_{kl}$  [47], with  $\varepsilon = \frac{1}{2}[\nabla \mathbf{u} + (\nabla \mathbf{u})^T]$  and  $\nabla \mathbf{w}$  the phononic and phasonic strains, respectively. The elastic constants  $\mathbf{C}$ ,  $\mathbf{K}$ , and  $\mathbf{R}' = \mathbf{R}^T$  thus result

$$\begin{aligned} C_{ijkl} &= 8A\phi_0^2 \sum_{n=1}^N G_{n,i}^{\parallel} G_{n,j}^{\parallel} G_{n,k}^{\parallel} G_{n,l}^{\parallel}, \\ R_{ijkl} &= 16A\phi_0^2 \sum_{n=1}^N G_{n,i}^{\parallel} G_{n,j}^{\parallel} G_{n,k}^{\parallel} G_{n,l}^{\perp}, \\ K_{ijkl} &= 16A\phi_0^2 \sum_{n=1}^N G_{n,i}^{\parallel} G_{n,j}^{\perp} G_{n,k}^{\parallel} G_{n,l}^{\perp}. \end{aligned} \quad (7)$$

consistent with known results for QCs [25, 47]. For instance, for decagonal QCs,  $C_{ijkl} = \lambda \delta_{ij} \delta_{kl} + 2\mu(\delta_{ik} \delta_{jl} + \delta_{il} \delta_{jk})$  with  $\mu = \lambda = 5A\phi_0^2$  (isotropic, with a ratio close to experiments, e.g. for Al-Ni-Co QCs [48]),  $K_{ijkl} = K_1 \delta_{ik} \delta_{jl} + K_2(\delta_{ij} \delta_{kl} - \delta_{il} \delta_{jk})$  with  $K_1 = 10(3 + \sqrt{5})A\phi_0^2$  and  $K_2 = 0$ , and  $R_{1111} = R_{1122} = -R_{2211} = -R_{2222} = R_{1221} = R_{2121} = -R_{1212} = -R_{2112} = 5(1 + \sqrt{5})$ , and 0 elsewhere [47].

The description of defects and deformations is further showcased in Fig. 3, reporting the growth and impingement of two misoriented QCs (rotated  $\pm\alpha$ ), recently investigated in experiments [49]. A representative stage during growth is illustrated in Fig. 3a. From the phases  $\theta_n$ , we can determine the (4D) Burgers vectors  $\mathbf{b} = \mathbf{b}^{\parallel} \oplus \mathbf{b}^{\perp}$ . Defects with (five) different orientations form, having two Burgers vector lengths:  $|\tilde{\mathbf{b}}_1|^2 = \frac{16}{25}(5 - \sqrt{5})\pi^2$  for the lowest-energy defects, and  $|\tilde{\mathbf{b}}_2|^2 = \frac{24}{25}(5 - \sqrt{5})\pi^2$  for the second-lowest energy. Moreover, stress fields computed via Eq. (6) are consistent with the ones obtained by deriving analytic displacements [50] and multiplying by elastic constants (7) for the same Burgers vectors (see the SM [45]).

For periodic crystals, a straight semi-coherent interface hosting dislocations of the same kind is expected in the setting of Fig. 3a (see, e.g., Ref. [51]). A significantly different scenario thus emerges for QCs. Inherent phasonic deformations, absent in the initial rotation, are induced by defects as described by Eq. (4). Moreover, a rotation by  $-3\alpha$  in  $\Omega^{\perp}$  would be required to rotate the subspaces in a synchronized manner; we recall that  $\mathbf{G}_n^{\perp} \propto \mathbf{G}_{(3n \bmod 5)}^{\parallel}$ . A  $\Omega^{\parallel}$  rotation of the QCs thus introduces a geometric frustration, accommodated by the nucleation of defects of different kinds and arranged over a more complex network [52]. For comparison, Fig. 3b shows that a straight, semi-coherent interface composed of defects of the same kind is indeed obtained by the additional  $-3\alpha$  rotation in  $\Omega^{\perp}$ . However, this setting does not correspond to a physical rotation of the QCs in  $\Omega^{\parallel}$ , as it is visible in the inset in 3c, which deviates from a simple rotation of the structure in Fig. 1c. Due to such

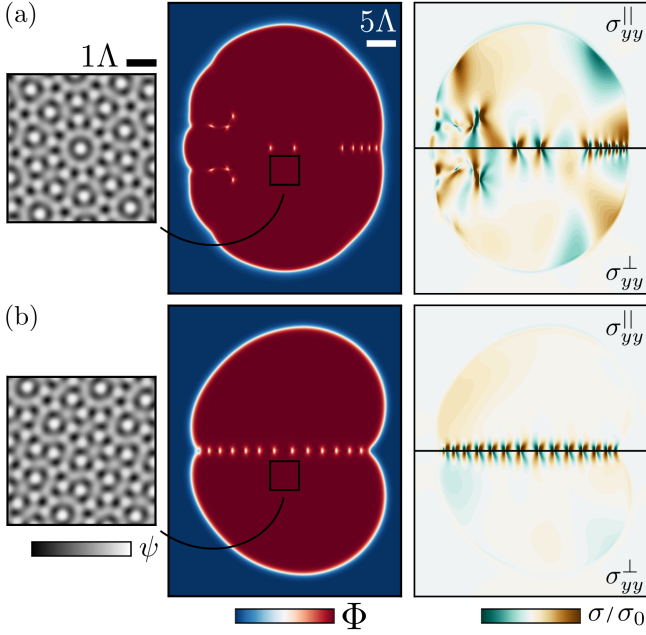


FIG. 3. *QC growth and semicoherent interfaces.* (a) Representative stage of the growth of two misoriented circular seeds ( $\alpha = \pm 4^\circ$  set as Fig. 2) with radius  $4\Lambda$  and center-to-center distance of  $9\Lambda$  along the  $y$ -axis. (b) Growth as in (a) with an additional rotation  $-3\alpha$  in  $\Omega^\perp$ . Parameters as in Fig. 2.

a nontrivial phononic-phasonic deformation, the orientations of the QCs are also varying, qualitatively reproducing the evidence in [49], and nucleation of additional defects at the surface occur at later stages, reminiscent of rearrangements mediated by phasons [37, 53].

Finally, we show that the proposed field theory also captures self-consistently the driving force for dislocation motion. Following the theoretical framework proposed for crystals [54–56], we can track Burgers vector densities  $\mathbf{B}^S$  for a dislocation at  $\mathbf{r}_0$  via the zeros of  $\eta_n$  corresponding to singularities in the phases  $\theta_n$ . In particular, we may express  $\mathbf{B}^S$  as superposition of Dirac-delta distributions  $\delta(\eta_n)$ ,

$$\mathbf{B}^\parallel = \mathbf{b}^\parallel \delta(\mathbf{r} - \mathbf{r}_0) = -\frac{4\pi}{N|\mathbf{b}^\parallel|^2} \sum_{n=1}^N \mathbf{G}_n^\parallel D_n \delta(\eta_n), \quad (8)$$

and  $\mathbf{B}^\perp = (|\mathbf{b}^\parallel|^2/|\mathbf{b}^\perp|^2)\mathbf{B}^\parallel$ , following from Eq. (5) upon contracting with  $\mathbf{G}_n^S$ .  $D_n = \frac{\epsilon_{jk}}{2i} \partial_j \eta_n^* \partial_k \eta_n$  is the determinant of the coordinate transformation from  $\mathbf{r}$  to  $(\text{Re}(\eta_n), \text{Im}(\eta_n))$  [57].  $\mathbf{B}^S$  and  $D_n$  follow the continuity equations  $\partial_t D_n + \partial_j J_{n,j}^D = 0$  and  $\partial_t B_i^S + \partial_j J_{i,j}^{B,S} = 0$ , with conservative current densities given by  $J_{n,j}^D = \epsilon_{jk} \text{Im}(\partial_t \eta_n \partial_k \eta_n^*)$  and  $J_{i,j}^{B,S} = b_i^S v_j^S \delta(\mathbf{r} - \mathbf{r}_0)$  [58], and  $\mathbf{v}^S$  the dislocation velocity. Combining these equations and Eq. (8) we can determine explicitly the dislocation veloc-

ity from  $\mathbf{J}_n^D$  and thus  $\{\eta_n\}$ ,

$$v_i^S = \frac{4\pi}{N|\mathbf{b}^S|^2} \sum_{n=1}^N \mathbf{b}^S \cdot \mathbf{G}_n^S \frac{s_n J_{n,i}^D(\mathbf{r}_0)}{D_n(\mathbf{r}_0)}. \quad (9)$$

As  $\mathbf{b}^\perp \cdot \mathbf{G}_n^\perp = 2\pi - \mathbf{b}^\parallel \cdot \mathbf{G}_n^\parallel$  (Eq. (5) with  $s_n = 1$ ), it follows that there is also a constraint of the defect velocities in each subspace, namely that  $\mathbf{v}^\perp |\mathbf{b}^\perp|^2 + \mathbf{v}^\parallel |\mathbf{b}^\parallel|^2 = (8\pi^2/N) \sum_{n=1}^N \mathbf{J}_n^D/D_n$ . Evaluating the density current  $\mathbf{J}_n^D$  at  $\mathbf{r}_0$  means evaluating  $\partial_t \eta_n|_{\mathbf{r}=\mathbf{r}_0} \approx A \mathcal{G}^2 \eta_n|_{\mathbf{r}=\mathbf{r}_0}$  from Eq. (3) with  $\zeta_k|_{\mathbf{r}=\mathbf{r}_0} = 0$  due to amplitudes  $\eta_n$  vanishing at the core for  $s_n \neq 0$  [56]. By approximating the singular part of the phase  $\theta_n$  with the isotropic vortex ansatz  $s_n \arctan(y/x)$  [55, 59], and considering  $\mathbf{v}^\perp = \mathbf{v}^\parallel = \mathbf{v}$  [60], we obtain a Peach-Koehler (PK) type equation

$$v_i = M f_i^{\text{PK}} = \frac{5A}{\pi} \epsilon_{ij} \left( \sigma_{jk}^\parallel b_k^\parallel + a^2 \sigma_{jk}^\perp b_k^\perp \right), \quad (10)$$

with  $M = 5A/\pi$ , retaining a dependence on both phononic and phasonic deformation consistent with classical theories [60, 61]. We refer to the SM [45] for the full derivation.

An example of the PK force field evaluation is illustrated in Fig. 4. We compute  $\mathbf{f}_{\text{PK}}$  acting on a test dislocation with Burgers vector  $\mathbf{b}^\parallel = \mathbf{b}^\perp = (0, \frac{8}{5}\pi \sin(\frac{4}{5}\pi))$  and that is induced by stress field of an opposite-charged dislocation located at the origin. We report the result obtained by using the stress field computed from  $\{\eta_n\}$  via Eq. (6) (*numerical*) and, for comparison, the prediction exploiting analytic displacements in Ref. [50] (*analytic*); see further details in the caption [45]. Given a distribution of dislocations, we can then compute the PK force field following from the symmetry of the QCs only.

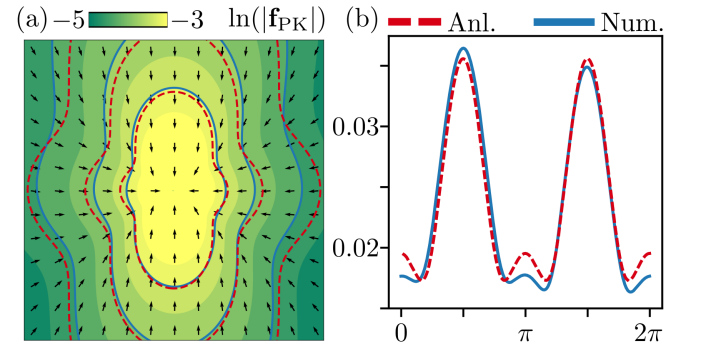


FIG. 4. *Peach-Koehler force for selected dislocations in a decagonal QC.* (a)  $\mathbf{f}_{\text{PK}}$  from Eq. (10), generated by a dislocation at the center of the panel on a test dislocation with opposite Burgers vector. Direction (arrows) and magnitude (color map and solid isolines) are obtained with the stress field computed by Eq. (6) (*Num.*). Dashed isolines are obtained with stress obtained via analytical displacements in [50] and elastic constants (7) (*Anl.*). (b) Comparison between *Num.* (solid) and *Anl.* (dashed)  $|\mathbf{f}_{\text{PK}}|$  varying the polar angle at a distance  $5\Lambda$  from the center of panel (a).



Moreover, the compelling agreement between the *numerical* and *analytical* force fields further supports the consistency of the elasticity description for QCs achieved in the proposed theory with continuum mechanics, while simultaneously capturing mesoscale aspects like defect formation and interaction with no additional tuning parameters.

In summary, the proposed mesoscale field theory builds on the density-wave description of QCs. It focuses on the slowly-varying complex amplitudes of the characteristic Fourier modes of the microscopic density field. A free energy functional for these amplitudes is introduced. This newly proposed theory may be considered a mesoscale Landau theory for phase transition in QCs, including mechanics. Elasticity and dislocations, including phononic and phasonic deformations, follow from the symmetry of the microscopic quasicrystalline order and are shown to be consistent with classical continuum mechanics results. Using this approach, we shed light on the formation of semi-coherent interfaces between mis-oriented QCs. Dislocation kinematics is also shown to follow from the proposed equation of motion for the amplitude. A self-consistent connection between micro- and macroscopic length scales in QCs is thus established. We expect this theory to pave the way for general mesoscale investigations of systems with quasicrystalline order.

M. D. D. and M. S. acknowledge the support from the German Research Foundation (DFG) under Grant SA4032/2-1 (Project No. 447241406) and the computing time made available to them on the high-performance computer at the NHR Center of TU Dresden. K. R. E. acknowledges support from the National Science Foundation (NSF) under Grant No. DMR-2006456.

---

\* [marco.salvalaglio@tu-dresden.de](mailto:marco.salvalaglio@tu-dresden.de)

- [1] D. Levine and P. J. Steinhardt, Quasicrystals: A new class of ordered structures, *Phys. Rev. Lett.* **53**, 2477 (1984).
- [2] D. Shechtman, I. Blech, D. Gratias, and J. W. Cahn, Metallic phase with long-range orientational order and no translational symmetry, *Phys. Rev. Lett.* **53**, 1951 (1984).
- [3] T. Ishimasa, H.-U. Nissen, and Y. Fukano, New ordered state between crystalline and amorphous in ni-cr particles, *Phys. Rev. Lett.* **55**, 511 (1985).
- [4] D. D. P and P. J. Steinhardt, *Quasicrystals: The State of the Art* (World Scientific, Singapore, 1991).
- [5] C. Janot, *Quasicrystals: A primer* (Oxford University Press, UK, 1994).
- [6] L. Bindi, P. J. Steinhardt, N. Yao, and P. J. Lu, Natural quasicrystals, *Science* **324**, 1306 (2009).
- [7] E. Maciá, The role of aperiodic order in science and technology, *Rep. Prog. Phys.* **69**, 397 (2005).
- [8] J.-M. Dubois, Properties and applications of quasicrystals and complex metallic alloys, *Chemical Society Reviews* **41**, 6760 (2012).
- [9] X. Zeng, G. Ungar, Y. Liu, V. Percec, A. E. Dulcey, and J. K. Hobbs, Supramolecular dendritic liquid quasicrystals, *Nature* **428**, 157 (2004).
- [10] K. Hayashida, T. Dotera, A. Takano, and Y. Matsushita, Polymeric quasicrystal: Mesoscopic quasicrystalline tiling in *abc* star polymers, *Phys. Rev. Lett.* **98**, 195502 (2007).
- [11] D. V. Talapin, E. V. Shevchenko, M. I. Bodnarchuk, X. Ye, J. Chen, and C. B. Murray, Quasicrystalline order in self-assembled binary nanoparticle superlattices, *Nature* **461**, 964 (2009).
- [12] W. Steurer, Why are quasicrystals quasiperiodic?, *Chem. Soc. Rev.* **41**, 6719 (2012).
- [13] T. Dotera, Quasicrystals in soft matter, *Isr. J. Chem.* **51**, 1197 (2011).
- [14] J. Mikhael, J. Roth, L. Helden, and C. Bechinger, Archimedean-like tiling on decagonal quasicrystalline surfaces, *Nature* **454**, 501 (2008).
- [15] S. Förster, K. Meinel, R. Hammer, M. Trautmann, and W. Widdra, Quasicrystalline structure formation in a classical crystalline thin-film system, *Nature* **502**, 215 (2013).
- [16] R. Penrose, The role of aesthetics in pure and applied mathematical research, *Bull. Inst. Math. Appl.* **10**, 266 (1974).
- [17] P. J. Lu and P. J. Steinhardt, Decagonal and quasicrystalline tilings in medieval islamic architecture, *Science* **315**, 1106 (2007).
- [18] A. Plati, R. Maire, E. Fayen, F. Boulogne, F. Restagno, F. Smalenburg, and G. Foffi, Quasi-crystalline order in vibrating granular matter, *Nat. Phys.* **20**, 465 (2024).
- [19] F. Mivehvar, H. Ritsch, and F. Piazza, Emergent quasicrystalline symmetry in light-induced quantum phase transitions, *Phys. Rev. Lett.* **123**, 210604 (2019).
- [20] J. E. S. Socolar, T. C. Lubensky, and P. J. Steinhardt, Phonons, phasons, and dislocations in quasicrystals, *Phys. Rev. B* **34**, 3345 (1986).
- [21] P. Bak, Icosahedral crystals: Where are the atoms?, *Phys. Rev. Lett.* **56**, 861 (1986).
- [22] P. Guyot, Dislocations in quasicrystals, *Encyclopedia of Materials: Science and Technology*, 2291 (2001).
- [23] L. Bendersky, Quasicrystal with one-dimensional translational symmetry and a tenfold rotation axis, *Phys. Rev. Lett.* **55**, 1461 (1985).
- [24] Discrete diffraction diagrams became the defining property of crystals by the International Union of Crystallography since 1992, fostered by the discovery of QCs [62].
- [25] D. Levine, T. C. Lubensky, S. Ostlund, S. Ramaswamy, P. J. Steinhardt, and J. Toner, Elasticity and dislocations in pentagonal and icosahedral quasicrystals, *Phys. Rev. Lett.* **54**, 1520 (1985).
- [26] Note that the formulation in (1) with c.c. accounts for  $\pm \mathbf{G}_n \forall n$ .
- [27] N. D. Mermin and S. M. Troian, Mean-field theory of quasicrystalline order, *Phys. Rev. Lett.* **54**, 1524 (1985).
- [28] R. Lifshitz and D. M. Petrich, Theoretical model for faraday waves with multiple-frequency forcing, *Phys. Rev. Lett.* **79**, 1261 (1997).
- [29] J. Swift and P. C. Hohenberg, Hydrodynamic fluctuations at the convective instability, *Phys. Rev. A* **15**, 319 (1977).
- [30] M. C. Cross and P. C. Hohenberg, Pattern formation outside of equilibrium, *Rev. Mod. Phys.* **65**, 851 (1993).
- [31] K. R. Elder, M. Katakowski, M. Haataja, and M. Grant, Modeling Elasticity in Crystal Growth, *Phys. Rev. Lett.*

- 88**, 245701 (2002).
- [32] T. V. Ramakrishnan and M. Yussouff, First-principles order-parameter theory of freezing, *Phys. Rev. B* **19**, 2775 (1979).
- [33] H. L. Michael te Vrugt and R. Wittkowski, Classical dynamical density functional theory: from fundamentals to applications, *Advances in Physics* **69**, 121 (2020).
- [34] K. Barkan, H. Diamant, and R. Lifshitz, Stability of quasicrystals composed of soft isotropic particles, *Phys. Rev. B* **83**, 172201 (2011).
- [35] J. Rottler, M. Greenwood, and B. Ziebarth, Morphology of monolayer films on quasicrystalline surfaces from the phase field crystal model, *J. Phys. Cond. Matter* **24**, 135002 (2012).
- [36] A. J. Archer, A. M. Rucklidge, and E. Knobloch, Quasicrystalline order and a crystal-liquid state in a soft-core fluid, *Phys. Rev. Lett.* **111**, 165501 (2013).
- [37] C. V. Achim, M. Schmiedeberg, and H. Löwen, Growth modes of quasicrystals, *Phys. Rev. Lett.* **112**, 255501 (2014).
- [38] K. Barkan, M. Engel, and R. Lifshitz, Controlled self-assembly of periodic and aperiodic cluster crystals, *Phys. Rev. Lett.* **113**, 098304 (2014).
- [39] Q. Xue, S.-a. Gong, and S. Tang, Atomic-scale investigation of the pattern formation of quasicrystal growth by phase-field crystal simulations, *Cryst. Growth Des* **22**, 5497 (2022).
- [40] N. Goldenfeld, B. P. Athreya, and J. A. Dantzig, Renormalization group approach to multiscale simulation of polycrystalline materials using the phase field crystal model, *Phys. Rev. E* **72**, 020601(R) (2005).
- [41] M. Salvalaglio, A. Voigt, and K. R. Elder, Closing the gap between atomic-scale lattice deformations and continuum elasticity, *npj Comput. Mater.* **5**, 48 (2019).
- [42] M. Salvalaglio and K. R. Elder, Coarse-grained modeling of crystals by the amplitude expansion of the phase-field crystal model: an overview, *Model. Simul. Mater. Sci. Eng.* **30**, 053001 (2022).
- [43] J. E. S. Socolar and P. J. Steinhardt, Quasicrystals. ii. unit-cell configurations, *Phys. Rev. B* **34**, 617 (1986).
- [44] P. J. Steinhardt, H.-C. Jeong, K. Saitoh, M. Tanaka, E. Abe, and A. Tsai, Experimental verification of the quasi-unit-cell model of quasicrystal structure, *Nature* **396**, 55 (1998).
- [45] See supplemental material (SM) for: a review of the definitions of  $\mathcal{L}$  and  $\mathbf{G}_n^{\parallel}, \mathbf{G}_n^{\perp}$  for decagonal QCs; details for the determination of  $\Lambda$  and the tiling; full expressions for the free energy for decagonal and icosahedral QCs; all derivation steps for strain and stress fields as well as dislocation velocity equations; numerical methods. SM includes Refs. [63–65].
- [46] D.-H. Yeon, Z.-F. Huang, K. R. Elder, and K. Thornton, Density-amplitude formulation of the phase-field crystal model for two-phase coexistence in two and three dimensions, *Phil. Mag.* **90**, 237 (2010).
- [47] D. H. Ding, W. Yang, C. Hu, and R. Wang, Generalized elasticity theory of quasicrystals, *Phys. Rev. B* **48**, 7003 (1993).
- [48] M. A. Chernikov, H. R. Ott, A. Bianchi, A. Migliori, and T. W. Darling, Elastic moduli of a single quasicrystal of decagonal al-ni-co: Evidence for transverse elastic isotropy, *Phys. Rev. Lett.* **80**, 321 (1998).
- [49] I. Han, K. L. Wang, A. T. Cadotte, Z. Xi, H. Parsamehr, X. Xiao, S. C. Glotzer, and A. J. Shahani, Formation of a single quasicrystal upon collision of multiple grains, *Nature Communications* **12**, 5790 (2021).
- [50] P. De and R. A. Pelcovits, Linear elasticity theory of pentagonal quasicrystals, *Phys. Rev. B* **35**, 8609 (1987).
- [51] S. Praetorius, M. Salvalaglio, and A. Voigt, An efficient numerical framework for the amplitude expansion of the phase-field crystal model, *Model. Simul. Mater. Sci. Eng.* **27**, 044004 (2019).
- [52] Y. Hatwalne, H. R. Krishnamurthy, R. Pandit, and S. Ramaswamy, Small-angle grain boundaries in quasicrystals, *Phys. Rev. Lett.* **62**, 2699 (1989).
- [53] K. Nagao, T. Inuzuka, K. Nishimoto, and K. Edagawa, Experimental observation of quasicrystal growth, *Phys. Rev. Lett.* **115**, 075501 (2015).
- [54] A. Skaugen, L. Angheluta, and J. Viñals, Dislocation dynamics and crystal plasticity in the phase-field crystal model, *Phys. Rev. B* **97**, 054113 (2018).
- [55] M. Salvalaglio, A. Voigt, Z.-F. Huang, and K. R. Elder, Mesoscale defect motion in binary systems: Effects of compositional strain and cottrell atmospheres, *Phys. Rev. Lett.* **126**, 185502 (2021).
- [56] V. Skogvoll, L. Angheluta, A. Skaugen, M. Salvalaglio, and J. Viñals, A phase field crystal theory of the kinematics of dislocation lines, *J. Mech. Phys. of Solids* **166**, 104932 (2022).
- [57] This holds true in 2D, see Ref [56] for extensions to 3D.
- [58] V. Skogvoll, J. Rønning, M. Salvalaglio, and L. Angheluta, A unified field theory of topological defects and non-linear local excitations, *npj Comput. Mater.* **9**, 122 (2023).
- [59] G. F. Mazenko, Vortex velocities in the  $O(n)$  symmetric time-dependent ginzburg-landau model, *Phys. Rev. Lett.* **78**, 401 (1997).
- [60] T. C. Lubensky, S. Ramaswamy, and J. Toner, Dislocation motion in quasicrystals and implications for macroscopic properties, *Phys. Rev. B* **33**, 7715 (1986).
- [61] E. Agiasofitou, M. Lazar, and H. Kirchner, Generalized dynamics of moving dislocations in quasicrystals, *J. Phys. Cond. Matter* **22**, 495401 (2010).
- [62] Report of the Executive Committee for 1991, *Acta Crystallographica Section A* **48**, 922 (1992).
- [63] P. Hirvonen, V. Heinonen, H. Dong, Z. Fan, K. R. Elder, and T. Ala-Nissila, Phase-field crystal model for heterostructures, *Phys. Rev. B* **100**, 165412 (2019).
- [64] V. Skogvoll, A. Skaugen, and L. Angheluta, Stress in ordered systems: Ginzburg-landau-type density field theory, *Phys. Rev. B* **103**, 224107 (2021).
- [65] L. Benoit-Maréchal and M. Salvalaglio, Gradient elasticity in Swift–Hohenberg and phase-field crystal models, *Model. Simul. Mater. Sci. Eng.* **32**, 055005 (2024).

# SUPPLEMENTAL MATERIAL

## Mesoscale Field Theory for Quasicrystals

Marcello De Donno,<sup>1</sup> Luiza Angheluta,<sup>2</sup> Ken R. Elder<sup>3</sup>, Marco Salvalaglio<sup>1,4,\*</sup>

<sup>1</sup>*Institute of Scientific Computing, TU Dresden, 01062 Dresden, Germany*

<sup>2</sup>*Njord Centre, Department of Physics, University of Oslo, 0371 Oslo, Norway*

<sup>3</sup>*Department of Physics, Oakland University, Rochester, Michigan 48309, USA*

<sup>4</sup>*Dresden Center for Computational Materials Science (DCMS), TU Dresden, 01062 Dresden, Germany*

### S-I. DEFINITIONS OF DIRECT- AND RECIPROCAL-SPACE VECTORS FOR DECAGONAL QUASICRYSTALS

In this work, we consider quasicrystals (QCs) described by the plane-wave expansion of the microscopic density field:

$$\psi = \psi_0 + \sum_n \eta_j e^{i\mathbf{G}_n \cdot \mathbf{r}} + \eta_j^* e^{-i\mathbf{G}_n \cdot \mathbf{r}}, \quad (\text{S-1})$$

where  $\mathbf{G}_n$  are reciprocal-lattice vectors producing the desired lattice structure and  $\psi_0$  the average density. Following seminal works for the decagonal quasicrystal (see, for instance, Ref. [S1]), we consider a four-dimensional periodic hyperlattice  $\mathcal{L}$ , which allows us to obtain the quasicrystalline arrangement upon projection on a two-dimensional subspace. The latter is the physical space of the definition of QCs and is called parallel space ( $\Omega^\parallel$ ). The additional dimensions to be considered to define the periodic hyperlattice form another subspace of  $\mathcal{L}$  called perpendicular space ( $\Omega^\perp$ ). We define five (four-dimensional) vectors  $\tilde{\mathbf{b}}_m \in \mathcal{L}$ , and five vectors  $\tilde{\mathbf{G}}_n$  belonging to its reciprocal lattice:

$$\begin{aligned} \tilde{\mathbf{b}}_m &= \mathbf{b}_m^\parallel \oplus b\mathbf{b}_m^\perp, & m = 0, \dots, 4 \\ \tilde{\mathbf{G}}_n &= \mathbf{G}_n^\parallel \oplus a\mathbf{G}_n^\perp, & n = 0, \dots, 4 \end{aligned} \quad (\text{S-2})$$

where  $\mathbf{b}_m^\parallel$  and  $\mathbf{b}_m^\perp$  are vectors in parallel and perpendicular space, and  $\mathbf{G}_n^\parallel$  and  $\mathbf{G}_n^\perp$  are vectors in their respective reciprocal spaces. The symbol  $\oplus$  represents vector concatenation. The coefficients  $a, b$  allow the vectors in parallel and perpendicular space to have different norms, and we will determine their values shortly.

Owing to the symmetry of decagonal QCs, the vectors in parallel space (direct and reciprocal) are

$$\begin{aligned} \mathbf{b}_m^\parallel &= r \begin{pmatrix} -\sin(2\pi m/5) \\ \cos(2\pi m/5) \end{pmatrix}, \\ \mathbf{G}_n^\parallel &= g \begin{pmatrix} \cos(2\pi n/5) \\ \sin(2\pi n/5) \end{pmatrix}, \end{aligned} \quad (\text{S-3})$$

with  $r, g$  the length of the vectors. The vectors in perpendicular space (direct and reciprocal) can be constructed by a simple re-indexing of those in parallel space:

$$\begin{aligned} \mathbf{b}_m^\perp &= \mathbf{b}_{3m}^\parallel, \\ \mathbf{G}_n^\perp &= \mathbf{G}_{3n}^\parallel. \end{aligned} \quad (\text{S-4})$$

We remark that, due to the periodicity of the sinusoids used to construct the vectors in Eq. (S-3), a modulo five operation is implied in all the indices in Eqs. (S-3, S-4), i.e.  $\mathbf{b}_{m+5i}^\parallel = \mathbf{b}_m^\parallel \forall i \in \mathbb{Z}$ , and the same for the other vectors. In order to determine the coefficients  $a, b, g, r$ , we define the phase

$$\begin{aligned} \tilde{\theta}_{n-m} &= \tilde{\mathbf{G}}_n \cdot \tilde{\mathbf{b}}_m \\ &= gr \left( \sin(2\pi(n-m)/5) + ab \sin(6\pi(n-m)/5) \right). \end{aligned} \quad (\text{S-5})$$

By imposing

$$\begin{cases} \theta_1 = \theta_4 = gr(\sin(2\pi/5) - ab \sin(4\pi/5)) \equiv 0, \\ \theta_2 = -\theta_3 = gr(\sin(4\pi/5) + ab \sin(2\pi/5)) \equiv 2\pi, \end{cases} \quad (\text{S-6})$$

we get

$$\begin{cases} ab = \frac{1}{2}(1 + \sqrt{5}), \\ gr = \frac{2\pi}{5}\sqrt{10 - 2\sqrt{5}}. \end{cases} \quad (\text{S-7})$$

We choose to take  $g = 1$ , meaning that the reciprocal lattice vectors in parallel space have unit length, as it is usual in (A)PFC models. We also take  $b = 1$ , meaning that the direct lattice vectors have the same length in both subspaces. Then, we are left with well-defined values for  $a$  and  $r$ , as determined in Eq. (S-7) with  $g = b = 1$ .

## S-II. DENSITY COARSE-GRAINING

Eq. (S-1) corresponds to an expansion in Fourier modes of the microscopic density field, which is used to define the amplitudes  $\{\eta_n\}$ . To obtain a free energy for the amplitudes from the one defined for the microscopic density, one needs to make sure that a characteristic volume exists over which variations of the density can be averaged out. See for instance the derivation of the APFC model from the PFC model [S2]. A coarse-graining procedure of any quantity can then be performed by averaging it over such representative volume element. For conventional crystals, the coarse-graining is straight-forward: the density is by definition periodic over the unit cell. Here, we show that the coarse-graining procedure can also be applied to the microscopic density of the decagonal QC, in agreement with the quasi-unit cell picture proposed in the literature [S3, S4].

We define the macroscopic (coarse-grained) density field  $\langle\psi\rangle$  as the average of  $\psi$  over some representative volume. This can be realized by the Gaussian convolution in 2D [S5, S6]:

$$\langle\psi\rangle(\mathbf{r}) = \int d\mathbf{r}' \frac{\psi(\mathbf{r}')}{2\pi\alpha^2} \exp\left(-\frac{(\mathbf{r} - \mathbf{r}')^2}{2\alpha^2}\right), \quad (\text{S-8})$$

where  $\alpha$  is the coarse-graining length. In Fig. S-1b, we report the results of the coarse-graining procedure for the density of a decagonal QC for different values of  $\alpha$ . We found that, for  $\alpha \sim 12.5932$ , the oscillations in the macroscopic density decrease by three orders of magnitudes with respect to the microscopic density. Interestingly, this value corresponds to the distance from the center of the QC of ten symmetric density maxima, two of which are shown in Fig. S-1a (see red dashed lines in  $\bar{\psi}(0, r)$  therein). The critical value  $\alpha \sim 12.5932$  is referred to as the coarsening length  $\Lambda$  in the main text. The existence of a (finite) coarsening length for the quasicrystal justifies the construction of free energy for the amplitudes in analogy to previous works on periodic crystals [S2], as detailed in Section S-IV.

## S-III. TILING

To obtain the tiling shown in Fig. 1 and 2 in the main text, we start from the density field reconstructed from the amplitudes according to Eq. (S-1). We numerically find all density maxima, and we discard those under an arbitrary threshold. We found that discarding maxima for which  $\psi/\psi_{\text{MAX}} < 0.5$  matches best other tiling representations of quasicrystals (see e.g. Ref. [S7]). The coordinates of the density maxima remaining after thresholding are then the coordinates of the vertices we plot.

The length of the tile edge is once again arbitrary, as the quasicrystal presents a distribution of interatomic distances with multiple sharp peaks in non-commensurate positions. In our description, a tiling matching those in literature, with edges connecting most neighboring vertices and with no crossing edges, is obtained by choosing an edge length  $l = 7.7 \pm 0.1$ . The same value was used for the relaxed quasicrystal in Fig. 1 and for the quasicrystal hosting defects in Fig. 2, resulting in broken edges for the latter.

## S-IV. FREE ENERGY

To illustrate more in detail the concepts underlying the free energy formulation for QCs introduced in the main text, we start with the Swift-Hohenberg energy functional used in the classical PFC description of conventional crystals,

$$F_\psi = \int_{\Omega} \left[ \frac{A}{2} \psi (q^2 + \nabla^2)^2 \psi + \frac{B}{2} \psi^2 + \frac{C}{3} \psi^3 + \frac{D}{4} \psi^4 \right] d\mathbf{r}, \quad (\text{S-9})$$



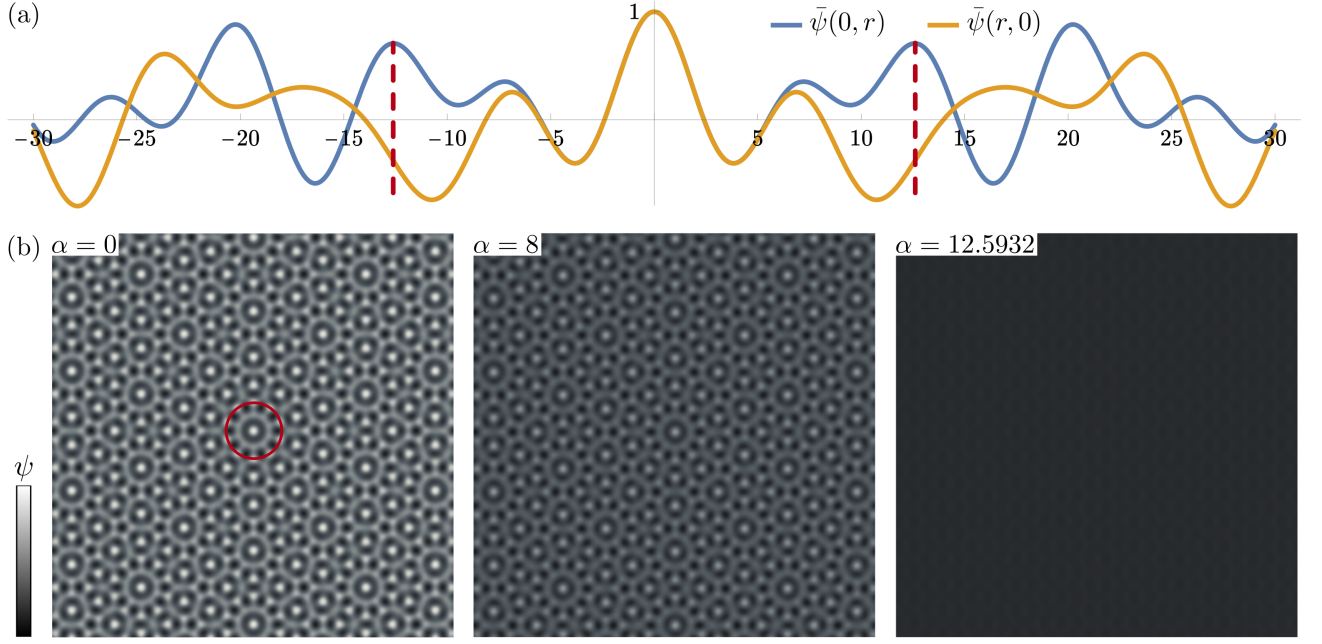


FIG. S-1. (a) Plot of the normalized density  $\bar{\psi} = \psi/\psi_{\text{MAX}}$  along the directions  $x = 0$  (blue) and  $y = 0$  (yellow), referred to as  $\bar{\psi}(0, r)$  and  $\bar{\psi}(r, 0)$ , respectively. The density peaks for  $\bar{\psi}(0, r)$  at  $y = \pm 12.5932$  are highlighted (see red dashed lines). (b) Plots of the coarse-grained density for different values of the standard deviation  $\alpha$  of the Gaussian kernel in Eq (S-8). A red circle with radius 12.5932 is drawn in the first panel.

with  $q$  the length of the principal wave vector for periodic minimizers of  $F_\psi$ . By using the amplitude expansion (S-1), one can derive a free energy functional  $F_\eta$  depending on  $\eta_j$  by a renormalization group approach or simply by substituting the expansion (S-1) into (S-9) and integrating over the unit cell [S2, S8],

$$F_\eta = \int_{\Omega} \left[ \sum_j A |\mathcal{G}_j \eta_j|^2 + B_2 \zeta_2 + B_3 \zeta_3 + B_4 \zeta_4 \right] d\mathbf{r}, \quad (\text{S-10})$$

with  $\mathcal{G}_j = \nabla^2 + 2i\mathbf{G}_j \cdot \nabla$ , and

$$\begin{aligned} \zeta_2 &= \sum_{p,q} \eta_p \eta_q \delta_{\mathbf{0}, \mathbf{G}_p + \mathbf{G}_q} = 2 \sum_{n=1}^N |\eta_n|^2 = \Phi, \\ \zeta_3 &= \sum_{p,q,r} \eta_p \eta_q \eta_r \delta_{\mathbf{0}, \mathbf{G}_p + \mathbf{G}_q + \mathbf{G}_r}, \\ \zeta_4 &= \sum_{p,q,r,s} \eta_p \eta_q \eta_r \eta_s \delta_{\mathbf{0}, \mathbf{G}_p + \mathbf{G}_q + \mathbf{G}_r + \mathbf{G}_s}. \end{aligned} \quad (\text{S-11})$$

where the summations are from  $-N$  to  $+N$  excluding zero,  $\eta_{-n} = \eta_n^*$ , and  $\mathbf{G}_{-n} = -\mathbf{G}_n$ . We remark the presence of the Kronecker delta in the definition above, meaning that the objects  $\zeta_l$  contain products of  $l$  amplitudes and their complex conjugate if and only if the vector sum of the corresponding reciprocal-space vectors ( $\mathbf{G}_n$ ) is zero. This is known as the resonance condition.

For quasicrystals, usually there exists no set of four or fewer  $\mathbf{G}_j$  whose sum is zero. See, for instance, when considering the reciprocal space vectors defined in Eq. (S-3). This causes the resonance conditions in Eqs. (S-11) to be never realized. Therefore, the QCs is not a stable phase of Eq. (S-9), with a stripe or a disordered phase being the global minima of the free energy depending on the parameters. A QC can be instead obtained by increasing the degree in the free energy polynomial so that combinations of more  $\mathbf{G}_j$  leading to resonance conditions can be considered. This concept traces back to the first theories of QCs for bulk systems [S9, S10]. For the decagonal or icosahedral quasicrystal, it is enough to increase the polynomial degree to six, which corresponds to retaining the next two higher order terms in the polynomial entering the non-local Swift-Hohenberg energy functional. We remark that

the highest order must be even to ensure the existence of a global minimum. The free energy density is then

$$F_\eta = \int_\Omega \left[ \sum_j A |\mathcal{G}_j \eta_j|^2 + B_2 \zeta_2 + B_3 \zeta_3 + B_4 \zeta_4 + B_5 \zeta_5 + B_6 \zeta_6 \right] d\mathbf{r}. \quad (\text{S-12})$$

With  $\zeta_5$  and  $\zeta_6$  obtained by extending the sums in Eq. (S-11) to product of five and six amplitudes, respectively.

For the decagonal quasicrystal defined as in Sect. S-I, the newly introduced terms read:

$$\begin{aligned} \zeta_5 &= \left( \prod_{j=1}^5 \eta_j \right) + \text{c.c.}, \\ \zeta_6 &= 720 \sum_{\substack{j>i \\ k>j}} |\eta_i|^2 |\eta_j|^2 |\eta_k|^2 + 180 \sum_{\substack{i \\ j \neq i}} |\eta_i|^4 |\eta_j|^2 + 20 \sum_i |\eta_i|^6. \end{aligned} \quad (\text{S-13})$$

With this addition to the free energy, the parameter space now contains a quasicrystal phase, but the stripe phase is still present. We found that, in general, a quasicrystal phase is obtained as global minimizer of the free energy when the parameter  $B_5$  is large and negative, and  $B_6$  is small and positive (see also Fig. 1 in the main text). Further, we remark that  $\zeta_3 = 0$  by construction, meaning that we can neglect  $B_3$ . The parameter set we use in the simulations reported in this work is  $A = 1$ ,  $B_2 = 0.02$ ,  $B_4 = 0$ ,  $B_5 = -100$ ,  $B_6 = 0.1$ .

For the icosahedral quasicrystal, we recall that the reciprocal lattice vectors are  $\mathbf{G}_n = (1/\sqrt{5})[2 \cos(2\pi n/5), 2 \sin(2\pi n/5), 1]$  for  $1 \leq n \leq 5$ , and  $\mathbf{G}_6 = [0, 0, 1]$  [S11]. Since we have six vectors, we can use the degree-six free energy, Eq. (S-12). We remark that there are no combinations of three or five  $\mathbf{G}_n$  with zero sum, meaning that  $\zeta_3 = \zeta_5 = 0$ . The definitions of  $\zeta_2$  and  $\zeta_4$  is the same as in Eq. (S-11). The definition of  $\zeta_6$  from Eq. (S-13) also holds, but it features an additional term reading

$$\zeta_6^S = \left( \prod_{j=1}^6 \eta_j \right) + \text{c.c.}, \quad (\text{S-14})$$

accounting for the fact that the sum of the six vectors  $\mathbf{G}_n$  is zero.

## S-V. NUMERICAL METHOD

In this section, we summarize the numerical method used to perform simulations. We recall the equation for the dynamics of the amplitudes we introduced in the main text

$$\partial_t \eta_n = -\frac{\delta F_\eta}{\delta \eta_n^*} = A \mathcal{G}_n^2 \eta_n + \sum_{k=2}^P B_k \partial_{\eta_n^*} \zeta_k, \quad (\text{S-15})$$

to be solved for each amplitude  $\eta_n$ . The first term on the right-hand side consists of an operator  $\mathcal{L}$  linear in the amplitude, while the second term is a non-linear polynomial  $\mathcal{N}$ . We can thus rewrite Eq. (S-15) as

$$\partial_t \eta_n = \mathcal{L} \eta_n + \mathcal{N}. \quad (\text{S-16})$$

This equation is solved by a Fourier pseudo-spectral method [S2]. In brief, we may consider the (discrete) Fourier transform of terms in Eq. (S-16) and rewrite the equation for the coefficient of the Fourier modes. This results in the equation

$$\partial_t [\widehat{\eta}_n]_k = \mathcal{L}_k [\widehat{\eta}_n]_k + [\widehat{\mathcal{N}}]_k, \quad (\text{S-17})$$

where  $[\widehat{\eta}_n]_k$  is the Fourier transform of the amplitudes,  $\mathcal{L}_k$  being a linear term is a simple algebraic expression of the Fourier space coordinates  $\mathbf{k}$  (for instance,  $[\widehat{\nabla^2 \eta_n}]_k = -|\mathbf{k}_n|^2 [\widehat{\eta}_n]_k$ ), and  $[\widehat{\mathcal{N}}]_k$  the Fourier transform of  $\mathcal{N}$ . Knowing  $\eta_n$  at time  $t$ , and thus its Fourier transform as well as  $[\widehat{\mathcal{N}}]_k$ , the amplitudes at the next timestep  $t + \Delta t$  are given by the following approximation

$$[\widehat{\eta}_n]_k(t + \Delta t) \approx [\widehat{\eta}_n]_k(t) \exp(\mathcal{L}_k \Delta t) + \frac{[\widehat{\mathcal{N}}]_k(t)}{\mathcal{L}_k} (\exp(\mathcal{L}_k \Delta t) - 1). \quad (\text{S-18})$$

We remark that the approximation is needed to account for the contribution of the non-linear part, while the linear term is exact. The solution in real space is then obtained by an inverse Fourier transform of  $[\hat{\eta}_n]_k$ . Our code is implemented in `python`, and it exploits the established Fast Fourier Transform algorithm FFTW [S12]. We use a timestep  $\Delta t = 1$ , and a uniform grid with ten mesh points per coarsening length  $\Lambda$ .

## S-VI. ENERGY VARIATION AND STRESS FIELDS

In this Section all the steps for deriving the stress fields for QCs, as discussed in the main text, are reported. The elastic energy is determined by the part of the free energy which depends on gradient of displacements fields (in both  $\Omega^{\parallel}$  and  $\Omega^{\perp}$  for QCs):

$$\mathcal{E} = A \int d\mathbf{r} \sum_{n=0}^4 |\mathcal{G}_n \eta_n|^2, \quad (\text{S-19})$$

where we can rewrite the differential operator as

$$\mathcal{G}_n = \nabla^2 + 2\mathbb{i}(\mathbf{G}_n \cdot \nabla) = \partial_j(\partial_j + 2\mathbb{i}G_{n,j}). \quad (\text{S-20})$$

The variational of the amplitudes with respect to an arbitrary phase variation  $\delta\theta_n$  is

$$\eta'_n = \eta_n e^{-\mathbb{i}\delta\theta_n} \approx \eta'_n = \eta_n(1 - \mathbb{i}\delta\theta_n) \rightarrow \delta\eta_n = -\mathbb{i}\eta_n \delta\theta_n. \quad (\text{S-21})$$

For infinitesimal phase variations, we then have the following relations between derivatives:

$$\begin{aligned} \partial_j \delta\eta_n &= -\mathbb{i}(\partial_j \eta_n) \delta\theta_n - \mathbb{i}\eta_n (\partial_j \delta\theta_n) \nabla^2 \delta\eta_n \\ &= -\mathbb{i}(\nabla^2 \eta_n) \delta\theta_n - 2\mathbb{i}(\partial_j \eta_n)(\partial_j \delta\theta_n) \mathcal{G}_n \delta\eta_n \\ &= -\mathbb{i}(\nabla^2 \eta_n) \delta\theta_n - 2\mathbb{i}(\partial_j \eta_n)(\partial_j \delta\theta_n) + 2(G_{n,j} \partial_j \eta_n) \delta\theta_n + 2\eta_n (G_{n,j} \partial_j \delta\theta_n). \end{aligned} \quad (\text{S-22})$$

By rearranging terms, we get

$$\mathcal{G}_n \delta\eta_n = -\mathbb{i}(\mathcal{G}_n \eta_n)(\delta\theta_n) - 2\mathbb{i}[(\partial_j + \mathbb{i}G_{n,j})\eta_n](\partial_j \delta\theta_n) = -\mathbb{i}(\mathcal{G}_n \eta_n)(\delta\theta_n) - 2\mathbb{i}(\mathcal{Q}_{n,j} \eta_n)(\partial_j \delta\theta_n), \quad (\text{S-23})$$

where  $\mathcal{Q}_{n,j} = \partial_j + \mathbb{i}G_{n,j}$ .

The variational of the elastic energy with respect to amplitude variations can be then written as

$$\delta\mathcal{E} = A \sum_{n=0}^4 \int d\mathbf{r} [(\mathcal{G}_n \eta_n)(\mathcal{G}_n^* \delta\eta_n^*) + (\mathcal{G}_n \delta\eta_n)(\mathcal{G}_n^* \eta_n^*)] = 2A \sum_{n=0}^4 \int d\mathbf{r} \text{Re} [(\mathcal{G}_n^* \eta_n^*)(\mathcal{G}_n \delta\eta_n)]. \quad (\text{S-24})$$

By using the identities reported above,

$$\begin{aligned} (\mathcal{G}_n^* \eta_n^*)(\mathcal{G}_n \delta\eta_n) &= -\mathbb{i}(\mathcal{G}_n^* \eta_n^*)(\mathcal{G}_n \eta_n)(\delta\theta_n) - 2\mathbb{i}(\mathcal{G}_n^* \eta_n^*)(\mathcal{Q}_{n,j} \eta_n)(\partial_j \delta\theta_n) \\ &= -\mathbb{i}|\mathcal{G}_n \eta_n|^2 (\delta\theta_n) - 2\mathbb{i}(\mathcal{G}_n^* \eta_n^*)(\mathcal{Q}_{n,j} \eta_n)(\partial_j \delta\theta_n). \end{aligned} \quad (\text{S-25})$$

The first term is purely imaginary. Therefore, only the second term contributes to (S-24), and

$$\text{Re} [(\mathcal{G}_n^* \eta_n^*)(\mathcal{G}_n \delta\eta_n)] = 2 \text{Im} [(\mathcal{G}_n^* \eta_n^*)(\mathcal{Q}_{n,j} \eta_n)] (\partial_j \delta\theta_n). \quad (\text{S-26})$$

Thus, the variational of the elastic energy with respect to infinitesimal variations of the displacements is

$$\begin{aligned} \delta\mathcal{E} &= 4A \sum_{n=0}^4 \int d\mathbf{r} \text{Im} [(\mathcal{G}_n^* \eta_n^*)(\mathcal{Q}_{n,j} \eta_n)] (\partial_j \delta\theta_n) \\ &= 4A \sum_{n=0}^4 \int d\mathbf{r} \text{Im} [(\mathcal{G}_n^* \eta_n^*)(\mathcal{Q}_{n,j} \eta_n)] \left( G_{n,i}^{\parallel} \partial_j \delta u_i + G_{n,i}^{\perp} \partial_j \delta w_i \right). \end{aligned} \quad (\text{S-27})$$

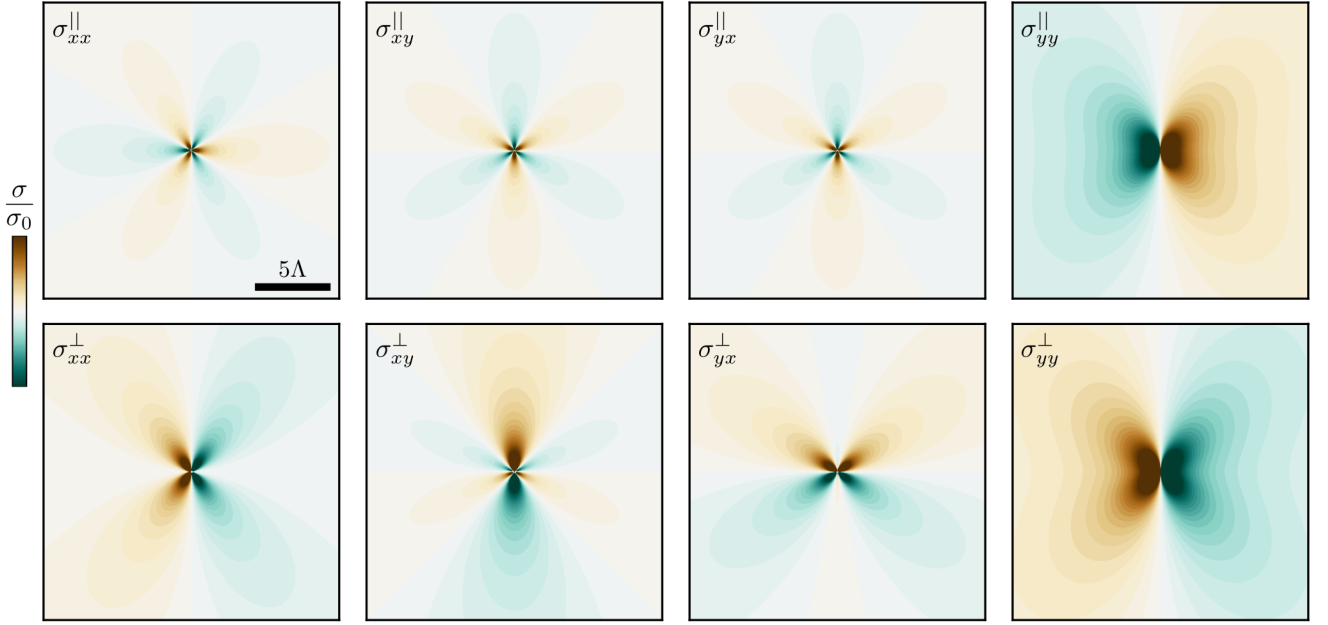


FIG. S-2. Components of the analytical stress field, Eqs. (S-32) and (S-33), for a dislocation with the Burgers vector observed along the grain boundary in Fig. 3 in the main text. The Burgers vectors are:  $\mathbf{b}^{\parallel} = (0, \frac{2\pi}{5}\sqrt{2(\sqrt{5}+5)})$ ,  $\mathbf{b}^{\perp} = (0, -\frac{4\pi}{5}\sqrt{5-2\sqrt{5}})$ .

where  $\delta\mathbf{u}$  and  $\delta\mathbf{w}$  are the infinitesimal variations of the displacements in  $\Omega^{\parallel}$  and  $\Omega^{\perp}$  subspace respectively. Thus, following from the definition of stress fields  $\sigma_{ij}^{\parallel} = \delta F / \delta \partial_j u_i$  and  $\sigma_{ij}^{\perp} = \delta F / \delta \partial_j w_i$ , we obtain

$$\begin{aligned}\sigma_{ij}^{\parallel} &= 4A \sum_{n=0}^4 G_{n,i}^{\parallel} \text{Im}[(\mathcal{G}_n^* \eta_n^*)(\mathcal{Q}_{n,j} \eta_n)], \\ \sigma_{ij}^{\perp} &= 4A \sum_{n=0}^4 G_{n,i}^{\perp} \text{Im}[(\mathcal{G}_n^* \eta_n^*)(\mathcal{Q}_{n,j} \eta_n)],\end{aligned}\tag{S-28}$$

as reported in the main text, with the lowest order term reducing to the linear stress-strain relation. We note that the general expression for the stress obtained by coarse-graining the stress of the PFC density [S2], instead of deriving it from the free energy depending on amplitudes, includes higher order terms w.r.t Eq. (S-28). However, it reduces to the fields considered here by neglecting the highest (fourth) order only, with the two equations thus delivering very similar estimations.

### Analytic stress fields

It is also possible to derive analytical expressions for the stress field, starting from the equations for the displacement reported in Ref. [S13]. In this work, the resulting expressions are used to assess the stress field of dislocations described by amplitudes (see below) and predictions in Fig. 4 of the main text. We consider a dislocation with Burgers vector  $\mathbf{b}^{\parallel}$  generating the displacement field  $\mathbf{u}$  in  $\Omega^{\parallel}$ , and Burgers vector  $\mathbf{b}^{\perp}$  generating the displacement field  $\mathbf{w}$  in  $\Omega^{\perp}$ . Then, we can express the strains as [S1, S14]

$$\epsilon_{ij}^{\parallel} = \frac{1}{2}(\partial_i u_j + \partial_j u_i), \quad \epsilon_{ij}^{\perp} = \partial_i w_j.\tag{S-29}$$

From these, we write the stresses as

$$\begin{aligned}\sigma_{ij}^{\parallel} &= C_{ijkl} \epsilon_{kl}^{\parallel} + R_{ijkl} \epsilon_{kl}^{\perp}, \\ \sigma_{ij}^{\perp} &= R_{kl ij} \epsilon_{kl}^{\parallel} + K_{ijkl} \epsilon_{kl}^{\perp},\end{aligned}\tag{S-30}$$



where we used the elastic constants reported in the main text:

$$\begin{aligned}
C_{ijkl} &= 8A\phi_0^2 \sum_{n=1}^N G_{n,i}^{\parallel} G_{n,j}^{\parallel} G_{n,k}^{\parallel} G_{n,l}^{\parallel}, \\
R_{ijkl} &= 16A\phi_0^2 \sum_{n=1}^N G_{n,i}^{\parallel} G_{n,j}^{\parallel} G_{n,k}^{\parallel} G_{n,l}^{\perp}, \\
K_{ijkl} &= 16A\phi_0^2 \sum_{n=1}^N G_{n,i}^{\parallel} G_{n,j}^{\perp} G_{n,k}^{\parallel} G_{n,l}^{\perp}.
\end{aligned} \tag{S-31}$$

We refer to the expressions for the stress field obtained this way as *analytic*. Here, we report their explicit definitions:

$$\begin{aligned}
\sigma_{xx}^{\parallel} &= \frac{5 \left( -8b_x^{\parallel} y (3x^2 + y^2) + 8b_y^{\parallel} x (x - y)(x + y) - 3(\sqrt{5} + 1) d_x^{\parallel} y (x^2 + y^2) + 3(\sqrt{5} + 1) d_y^{\parallel} x (x^2 + y^2) \right)}{96\pi (x^2 + y^2)^2}, \\
\sigma_{xy}^{\parallel} = \sigma_{yx}^{\parallel} &= \frac{5 \left( 8b_x^{\parallel} x (x - y)(x + y) + 8b_y^{\parallel} y (x - y)(x + y) - 3(\sqrt{5} + 1) d_x^{\parallel} x (x^2 + y^2) - 3(\sqrt{5} + 1) d_y^{\parallel} y (x^2 + y^2) \right)}{96\pi (x^2 + y^2)^2}, \\
\sigma_{yy}^{\parallel} &= \frac{5 \left( 8b_x^{\parallel} y (x - y)(x + y) + 8b_y^{\parallel} (x^3 + 3xy^2) + 3(\sqrt{5} + 1) d_x^{\parallel} y (x^2 + y^2) - 3(\sqrt{5} + 1) d_y^{\parallel} x (x^2 + y^2) \right)}{96\pi (x^2 + y^2)^2},
\end{aligned} \tag{S-32}$$

and

$$\begin{aligned}
\sigma_{xx}^{\perp} &= -\frac{5y \left( 4(\sqrt{5} + 1) b_x^{\parallel} x^2 + 4(\sqrt{5} + 1) b_y^{\parallel} xy + 3(\sqrt{5} + 3) d_x^{\parallel} (x^2 + y^2) \right)}{48\pi (x^2 + y^2)^2}, \\
\sigma_{xy}^{\perp} &= \frac{5 \left( 2(\sqrt{5} + 1) (x - y)(x + y)(b_x^{\parallel} x + b_y^{\parallel} y) - 3(\sqrt{5} + 3) d_y^{\parallel} y (x^2 + y^2) \right)}{48\pi (x^2 + y^2)^2}, \\
\sigma_{yx}^{\perp} &= \frac{5 \left( 3(\sqrt{5} + 3) d_x^{\parallel} x (x^2 + y^2) - 2(\sqrt{5} + 1) (x - y)(x + y)(b_x^{\parallel} x + b_y^{\parallel} y) \right)}{48\pi (x^2 + y^2)^2}, \\
\sigma_{yy}^{\perp} &= \frac{5x \left( 3(\sqrt{5} + 3) d_y^{\parallel} (x^2 + y^2) - 4(\sqrt{5} + 1) y(b_x^{\parallel} x + b_y^{\parallel} y) \right)}{48\pi (x^2 + y^2)^2}.
\end{aligned} \tag{S-33}$$

In Fig. S-2 we plot the *analytic* stress components for a dislocation of the same type as those observed forming spontaneously along the grain boundary of the mismatched seeds in Fig. 3 in the main text. In Fig. S-3 we show the stress field for the setup used in Fig. 4 in the main text, a pair of dislocations with opposite Burgers vectors, with  $|\mathbf{b}^{\parallel}| = |\mathbf{b}^{\perp}| = (0, \frac{8}{5}\pi \sin(\frac{4}{5}\pi))$ . The stress field obtained numerically from Eq. (S-28) is found to match almost perfectly the analytic result from Eqs. (S-32)-(S-33).

## S-VII. STRAIN AND ROTATION FROM COMPLEX AMPLITUDES

To obtain expressions for strain and rotation fields as function of amplitudes we consider phonon and phason displacement,  $\mathbf{u}$  and  $\mathbf{w}$ , as recalled above. This displacement field determines the phases of amplitude functions as (see also the main text)

$$\eta_n = \phi_n \exp(-i\theta_n), \tag{S-34}$$

with  $\phi_n$  real constants corresponding to the value of the amplitudes in the relaxed bulk. In order to simplify the notation in this Section and the next, we redefine the amplitude phases from the main text as:

$$\theta_n = \mathbf{k}_n \cdot \mathbf{u} + a\mathbf{q}_n \cdot \mathbf{w}, \tag{S-35}$$

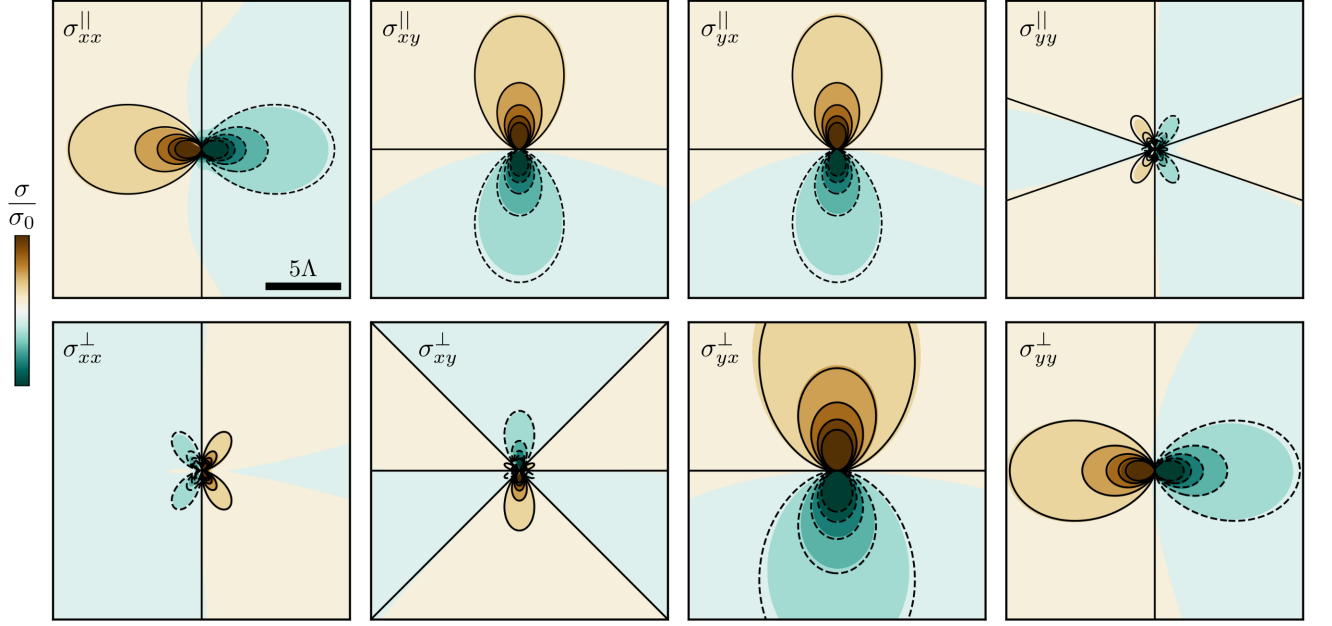


FIG. S-3. Components of the numerical stress field (color maps) compared with the analytical result (isolines) for a dislocation with Burgers vectors  $\mathbf{b}^|| = \mathbf{b}^\perp = (0, -\frac{8}{5}\pi \sin(\frac{4}{5}\pi))$ , the same used for Fig. 4 in the main text. Dashed isolines correspond to negative values. Further comparisons are shown in the main text, Fig. 4, illustrating that these elastic fields match very well also in terms of the driving force for defect motion.

so that  $\mathbf{k}_n = \mathbf{G}_n^||$ ,  $\mathbf{q}_n = \mathbf{G}_n^\perp$ , and  $a = (1 + \sqrt{5})/2$  the geometrical factor determined in Section S-I.

To determine the components of the displacement field  $u^x, u^y, w^x, w^y$ , we may invert equation (S-35) extending a procedure established for periodic crystal [S15]. We consider four amplitudes indexed by four (different) indexes  $l, m, n, o$  and rewrite the algebraic problem in matrix form

$$\begin{pmatrix} \theta_l \\ \theta_m \\ \theta_n \\ \theta_o \end{pmatrix} = \begin{pmatrix} k_l^x & k_l^y & a q_l^x & a q_l^y \\ k_m^x & k_m^y & a q_m^x & a q_m^y \\ k_n^x & k_n^y & a q_n^x & a q_n^y \\ k_o^x & k_o^y & a q_o^x & a q_o^y \end{pmatrix} \cdot \begin{pmatrix} u^x \\ u^y \\ w^x \\ w^y \end{pmatrix}, \quad (\text{S-36})$$

By solving such system of equations we obtain expressions for the components of the displacement fields

$$u^x = \frac{1}{\kappa_0} \left( \theta_o (k_l^y q_m^y q_n^x - q_l^y k_m^y q_n^x - k_l^y q_m^x q_n^y + q_l^x k_m^y q_n^y + q_l^y q_m^x k_n^y - q_l^x q_m^y k_n^y) + \right. \\ \theta_m (k_l^y q_n^y q_o^x + q_l^y q_n^x k_o^y - q_l^x q_n^y k_o^y - q_l^y k_n^y q_o^x - k_l^y q_n^x q_o^y + q_l^x k_n^y q_o^y) + \\ \theta_l (q_m^y k_n^y q_o^x + k_m^y q_n^x q_o^y + q_m^x q_n^y k_o^y - k_m^y q_n^y q_o^x - q_m^x k_n^y q_o^y - q_m^y q_n^x k_o^y) + \\ \left. \theta_n (-k_l^y q_m^y q_o^x + q_l^y k_m^y q_o^x + k_l^y q_m^x q_o^y - q_l^x k_m^y q_o^y - q_l^y q_m^x k_o^y + q_l^x q_m^y k_o^y), \right) \quad (\text{S-37})$$

$$u^y = \frac{-1}{\kappa_0} \left( \theta_o (k_l^x q_m^y q_n^x - q_l^x k_m^x q_n^x - k_l^x q_m^x q_n^y + q_l^x k_m^x q_n^y + q_l^y q_m^x k_n^x - q_l^x q_m^y k_n^x) + \right. \\ \theta_m (k_l^x q_n^y q_o^x + q_l^x q_n^x k_o^y + q_l^x k_n^x q_o^y - q_l^y k_n^x q_o^x - q_l^x q_n^y k_o^y - k_l^x q_n^x q_o^y) + \\ \theta_l (q_m^x q_n^y k_o^x + q_m^y k_n^x q_o^x + k_m^x q_n^x q_o^y - q_m^x k_n^x q_o^y - k_m^x q_n^y q_o^x - q_m^y q_n^x k_o^x) + \\ \left. \theta_n (-k_l^x q_m^y q_o^x + q_l^x k_m^x q_o^x + k_l^x q_m^x q_o^y - q_l^x k_m^x q_o^y - q_l^y q_m^x k_o^x + q_l^x q_m^y k_o^x), \right) \quad (\text{S-38})$$

$$w^x = \frac{1}{a\kappa_0} \left( \theta_o(k_l^y k_m^x q_n^y - k_l^x k_m^y q_n^y - k_l^y q_m^y k_n^x + q_l^y k_m^y k_n^x + k_l^x q_m^y k_n^y - q_l^y k_m^x k_n^y) + \right. \\ \theta_m(k_l^y k_n^x q_o^y + q_l^y k_n^y k_o^x + k_l^x q_n^y k_o^y - k_l^x k_n^y q_o^y - k_l^y q_n^y k_o^x - q_l^y k_n^x k_o^y) + \\ \theta_l(k_m^x k_n^y q_o^y + k_m^y q_n^y k_o^x + q_m^y k_n^x k_o^y - k_m^x k_n^x q_o^y - q_m^y k_n^y k_o^x - k_m^x q_n^y k_o^y) + \\ \left. \theta_n(-k_l^y k_m^x q_o^y + k_l^x k_m^y q_o^y + k_l^y q_m^y k_o^x - q_l^y k_m^y k_o^x - k_l^x q_m^y k_o^y + q_l^y k_m^x k_o^y) \right), \quad (\text{S-39})$$

$$w^y = \frac{1}{a\kappa_0} \left( \theta_o(-k_l^y k_m^x q_n^x + k_l^x k_m^y q_n^x + k_l^y q_m^x k_n^x - q_l^x k_m^y k_n^x - k_l^x q_m^x k_n^y + q_l^x k_m^x k_n^y) + \right. \\ \theta_m(k_l^x k_n^y q_o^x + k_l^y q_n^x k_o^x + q_l^x k_n^x k_o^y - k_l^x k_n^x q_o^x - q_l^x k_n^y k_o^x - k_l^x q_n^x k_o^y) + \\ \theta_l(k_m^y k_n^x q_o^x + q_m^x k_n^y k_o^x + k_m^x q_n^x k_o^y - k_m^x k_n^y q_o^x - k_m^y q_n^x k_o^x - q_m^x k_n^x k_o^y) + \\ \left. \theta_n(k_l^y k_m^x q_o^x - k_l^x k_m^y q_o^x - k_l^y q_m^x k_o^x + q_l^x k_m^y k_o^x + k_l^x q_m^x k_o^y - q_l^x k_m^x k_o^y) \right), \quad (\text{S-40})$$

with

$$\kappa_0 = \det \begin{vmatrix} k_l^x & k_l^y & q_l^x & q_l^y \\ k_m^x & k_m^y & q_m^x & q_m^y \\ k_n^x & k_n^y & q_n^x & q_n^y \\ k_o^x & k_o^y & q_o^x & q_o^y \end{vmatrix}. \quad (\text{S-41})$$

We remark that for the decagonal QC described via five amplitudes, one can construct five solutions to Eq. (S-36) as only four amplitudes are needed; however, these solutions are all equivalent.

From the expression of the displacement, we may obtain expressions for the strain field. We write the strain tensor in matrix form, implying  $\mathbf{u}$  does not depend on the perpendicular space coordinates, and vice-versa for the perpendicular space displacement  $\mathbf{w}$  [S13]:

$$\epsilon_{ij} = \begin{vmatrix} \epsilon_{xx}^{\parallel} & \epsilon_{xy}^{\parallel} & 0 & 0 \\ \epsilon_{yx}^{\parallel} & \epsilon_{yy}^{\parallel} & 0 & 0 \\ 0 & 0 & \epsilon_{xx}^{\perp} & \epsilon_{xy}^{\perp} \\ 0 & 0 & \epsilon_{yx}^{\perp} & \epsilon_{yy}^{\perp} \end{vmatrix}, \quad (\text{S-42})$$

where  $\epsilon_{ij}^{\parallel}$  and  $\epsilon_{ij}^{\perp}$  are the components of the strain in parallel and perpendicular space, respectively, defined as in agreement with the classical theory of elasticity in QCs [S1, S14] as in Eq. (S-29). The space-dependence of the displacements obtained by solving Eq. (S-36) is fully contained in the phases  $\theta_j$ . Therefore, spatial derivatives of displacements can be computed by using expressions analogous to (S-37)–(S-40) featuring  $\partial_i \theta_n$  terms instead of  $\theta_n$ . Derivatives of the phases can be generally computed as [S15]

$$\frac{\partial \theta_j}{\partial x_i} = \frac{1}{|\eta_j|^2} \left( \frac{\partial \text{Im}(\eta_j)}{\partial x_i} \text{Re}(\eta_j) - \frac{\partial \text{Re}(\eta_j)}{\partial x_i} \text{Im}(\eta_j) \right), \quad (\text{S-43})$$

from which strain tensor components can be expressed in terms of the amplitudes and reciprocal-lattice vectors only. For instance,

$$\epsilon_{xx}^{\parallel} = \partial_x u^x = \frac{1}{\kappa_0} \left( \partial_x \theta_o(k_l^y q_m^y q_n^x - q_l^y k_m^y q_n^x - k_l^y q_m^x q_n^y + q_l^x k_m^y q_n^y + q_l^y q_m^x k_n^y - q_l^x q_m^y k_n^y) + \right. \\ \partial_x \theta_m(k_l^y q_n^y q_o^x + q_l^y q_n^x k_o^y - q_l^x q_n^y k_o^y - q_l^y k_n^y q_o^x - k_l^y q_n^x q_o^y + q_l^x k_n^y q_o^y) + \\ \partial_x \theta_l(q_m^y k_n^y q_o^x + k_m^y q_n^x q_o^y + q_m^x q_n^y k_o^y - k_m^y q_n^y q_o^x - q_m^x k_n^y q_o^y - q_m^y q_n^x k_o^y) + \\ \left. \partial_x \theta_n(-k_l^y q_m^y q_o^x + q_l^y k_m^y q_o^x + k_l^y q_m^x q_o^y - q_l^x k_m^y q_o^y - q_l^y q_m^x k_o^y + q_l^x q_m^y k_o^y) \right), \quad (\text{S-44})$$

while other components of the strain tensor can be obtained by proceeding analogously with other expressions and/or derivatives. Note that the resulting strain components are continuously defined everywhere except at the core of dislocation, where, however, the effective elastic constants vanish, owing to integrable elastic energy (see also additional discussions for equations with a similar form in Ref. [S2, S15]).

Similarly, the rotation fields can be derived from amplitudes. Using the expressions for the displacement derived above, one can compute them according to the following definitions

$$\omega^{\parallel} = \nabla \times \mathbf{u}, \quad \omega^{\perp} = \nabla \times \mathbf{w}, \quad (\text{S-45})$$

representing rotations in  $\Omega^{\parallel}$  and  $\Omega^{\perp}$  (planes), respectively. For Fig. 2 in the main text, we selected the amplitude indices  $\{l, m, n, o\} = \{1, 2, 3, 4\}$ , resulting in:

$$\begin{aligned} \omega^{\parallel} &\sim 0.38 \partial_x(\theta_1 + 0.618\theta_2 - 0.618\theta_3 - \theta_4) + 0.276 \partial_y(\theta_1 + 2.618\theta_2 + 2.618\theta_3 + \theta_4), \\ \omega^{\perp} &\sim 0.145 \partial_x(\theta_1 + 1.618\theta_2 - 1.618\theta_3 - \theta_4) + 0.447 \partial_y(\theta_1 + 0.382\theta_2 + 0.382\theta_3 + \theta_4). \end{aligned} \quad (\text{S-46})$$

### S-VIII. DISLOCATION VELOCITY

In this section all the steps for deriving the velocity of dislocations in QCs are presented. We follow concepts introduced for periodic crystals, see Refs. [S16–S19], adapted here to QCs. A dislocation in crystals or QCs can be described via complex amplitudes  $\eta_n = |\eta_n|e^{i\theta_n}$  having singular phases  $\theta_n$  (so describing topological defects, with integer topological charges). The position of these singularities corresponds to the nominal core of the dislocations. At the singularity, the condition  $|\eta_n| = 0$  is realized, ensuring the integrability of the underlying free energy [S16]. Exploiting this concept, defects can then be tracked via superposition of Dirac-delta distributions  $\delta(\eta_n)$ . The Burgers vector density for a dislocation at  $\mathbf{r}_0 = \mathbf{0}$  has a distribution  $\propto \delta(\mathbf{r} - \mathbf{r}_0) = \delta(\mathbf{r})$ . In particular, starting from the definition of topological charge from the main text

$$\oint d\theta_n = -2\pi s_n = -(\mathbf{G}_n^{\parallel} \cdot \mathbf{b}^{\parallel} + \mathbf{G}_n^{\perp} \cdot \mathbf{b}^{\perp}), \quad (\text{S-47})$$

and contracting with  $\mathbf{G}_n^S$ , we may express the Burgers vector densities  $\mathbf{B}^S$  as superposition of Dirac-delta distributions  $\delta(\eta_n)$  [S17]

$$\begin{aligned} \mathbf{B}^{\parallel} &= \mathbf{b}^{\parallel} \delta(\mathbf{r} - \mathbf{r}_0) = -\frac{4\pi}{N|\mathbf{b}^{\parallel}|^2} \sum_{n=1}^N \mathbf{G}_n^{\parallel} D_n \delta(\eta_n), \\ \mathbf{B}^{\perp} &= \mathbf{b}^{\perp} \delta(\mathbf{r} - \mathbf{r}_0) = -\frac{4\pi}{N|\mathbf{b}^{\perp}|^2} \sum_{n=1}^N \mathbf{G}_n^{\perp} D_n \delta(\eta_n). \end{aligned} \quad (\text{S-48})$$

$D_n$  is the coordinate transformation between the (parallel) space coordinates and the components of the complex amplitudes, namely  $\text{Re}(\eta_n)$  and  $\text{Im}(\eta_n)$ .  $D_n$  plays the role of a smooth defect density field, and reads [S17–S19]

$$D_n = \frac{\epsilon_{jk}}{2i} \partial_j \eta_n^* \partial_k \eta_n. \quad (\text{S-49})$$

This is a conservative field, as its dynamic can be written in terms of a continuity equation

$$\partial_t D_n + \partial_j J_{n,j}^D = 0 \quad \text{with} \quad J_{n,j}^D = \epsilon_{jk} \text{Im}(\dot{\eta}_n \partial_k \eta_n^*). \quad (\text{S-50})$$

Considering general principles of conservation of topological charges, this must also hold for the Burgers vector density above, i.e.

$$\partial_t B_i^S + \partial_j J_{i,j}^{B,S} = 0 \quad \text{with} \quad J_{i,j}^{B,S} = b_i^S v_j^S \delta(\mathbf{r}). \quad (\text{S-51})$$

with  $S = \{\parallel, \perp\}$  and  $\mathbf{v}^S$  the velocity of the dislocation in the subspaces. By computing the time derivative of (S-48) expressed in terms of  $\delta(\eta_n)$  one gets

$$\begin{aligned} \frac{\partial B_i^S}{\partial t} &= -\frac{4\pi}{N} \sum_{n=1}^N G_{n,i}^S \left( \frac{\partial D_n}{\partial t} \delta(\eta_n) + D_n \frac{\partial}{\partial t} \delta(\eta_n) \right) \\ &= \frac{4\pi}{N} \sum_{n=1}^N G_{n,i}^S (\partial_j J_{n,j}^D \delta(\eta_n) + J_{n,j}^D \partial_j \delta(\eta_n)) \\ &= \partial_j \left( \frac{4\pi}{N} \sum_{n=1}^N G_{n,i}^S J_{n,j}^D \delta(\eta_n) \right), \end{aligned} \quad (\text{S-52})$$



The last expression can be used to identify  $J_{i,j}^{B,S}$  in terms of amplitudes (from  $\mathbf{J}_n^D$  and  $\delta(\eta_n)$ ). By equating this expression to  $J_{i,j}^{B,S}$  related to the velocity of the dislocation, Eq. (S-51), and expressing therein  $\delta(\mathbf{r})$  via the transformation in Eq. (S-48), one can then compute a general expression for the velocity  $\mathbf{v}^S$ :

$$v_j^S = \frac{4\pi}{N|\mathbf{b}^S|^2} \sum_{n=1}^N \mathbf{b}^S \cdot \mathbf{G}_n^S \frac{s_n J_{n,j}^D}{D_n} \Big|_{\mathbf{r}=\mathbf{0}}. \quad (\text{S-53})$$

with the specification at  $\mathbf{r} = \mathbf{0}$  (at the core of the dislocation) that follows from considering prefactor of delta functions, and we recall that  $\eta_n(\mathbf{r}) = 0$  for  $\mathbf{r} = \mathbf{0}$  when  $s_n \neq 0$ .

We now consider the specific case of a dislocation hosted in a decagonal QCs. We consider in general Burgers vectors corresponding to lattice vectors  $\mathbf{b}$  of the four-dimensional hyperlattice. For ease of notation, we redefine them so that  $\mathbf{b}_j = \mathbf{b}_j^{\parallel}$  and  $\mathbf{d}_j = \mathbf{b}_{3j}^{\parallel} = \mathbf{b}_j^{\perp}$  and we retain the notation  $\mathbf{k}_n = \mathbf{G}_n^{\parallel}$ ,  $\mathbf{q}_n = \mathbf{G}_n^{\perp}$  exploited in Sect. . We can then express the Burgers vector density fields, Eq. (S-48), of a dislocation with a given burgers vector  $(\mathbf{b}, \mathbf{d})$  as

$$\begin{aligned} b_j \delta(\mathbf{r}) &= -\frac{4\pi}{5} \sum_{n=0}^4 k_{n,j} D_n \delta(\eta_n), \\ d_j \delta(\mathbf{r}) &= -\frac{4\pi}{5a} \sum_{n=0}^4 q_{n,j} D_n \delta(\eta_n), \end{aligned} \quad (\text{S-54})$$

with velocities from Eq. (S-53):

$$\begin{aligned} v_j^{\parallel} &= \frac{4\pi}{5|\mathbf{b}|^2} \sum_{n=0}^4 \mathbf{b} \cdot \mathbf{k}_n \frac{s_n J_{n,j}^D}{D_n} \Big|_{\mathbf{r}=\mathbf{0}} = \frac{2}{5|\mathbf{b}|^2} \sum_{n=0}^4 \left( (\mathbf{b} \cdot \mathbf{k}_n)^2 + a(\mathbf{d} \cdot \mathbf{q}_n)(\mathbf{b} \cdot \mathbf{k}_n) \right) \frac{J_{n,j}^D}{D_n} \Big|_{\mathbf{r}=\mathbf{0}}, \\ v_j^{\perp} &= \frac{4\pi}{5a|\mathbf{d}|^2} \sum_{n=0}^4 \mathbf{d} \cdot \mathbf{q}_n \frac{s_n J_{n,j}^D}{D_n} \Big|_{\mathbf{r}=\mathbf{0}} = \frac{2}{5|\mathbf{d}|^2} \sum_{n=0}^4 \left( (\mathbf{d} \cdot \mathbf{q}_n)^2 + \frac{1}{a}(\mathbf{d} \cdot \mathbf{q}_n)(\mathbf{b} \cdot \mathbf{k}_n) \right) \frac{J_{n,j}^D}{D_n} \Big|_{\mathbf{r}=\mathbf{0}}, \end{aligned} \quad (\text{S-55})$$

where we used the definition  $s_n = \frac{1}{2\pi} (\mathbf{b} \cdot \mathbf{k}_n + a\mathbf{d} \cdot \mathbf{q}_n)$  introduced in the main text. According to the equations above, velocities may be different in parallel and perpendicular space. They are the same if the following identity holds:

$$\frac{1}{|\mathbf{b}|^2} \sum_{n=0}^4 \left( (\mathbf{b} \cdot \mathbf{k}_n)^2 + a(\mathbf{d} \cdot \mathbf{q}_n)(\mathbf{b} \cdot \mathbf{k}_n) \right) = \frac{1}{|\mathbf{d}|^2} \sum_{n=0}^4 \left( (\mathbf{d} \cdot \mathbf{q}_n)^2 + \frac{1}{a}(\mathbf{d} \cdot \mathbf{q}_n)(\mathbf{b} \cdot \mathbf{k}_n) \right). \quad (\text{S-56})$$

In the simulations reported in Fig. 3 in the main text, we observed dislocations with the lowest energy and with the second-lowest energy, for which  $|\mathbf{b} \oplus \mathbf{d}|^2 = \frac{16}{25}(5 - \sqrt{5})\pi^2$  and  $|\mathbf{b} \oplus \mathbf{d}|^2 = \frac{24}{25}(5 - \sqrt{5})\pi^2$  respectively. For these dislocations, condition (S-56) holds true, meaning that, for dislocations nucleating at interfaces between misoriented or mismatched interfaces, the condition  $\mathbf{v}^{\parallel} = \mathbf{v}^{\perp}$  holds. By exploiting the identity (S-56) we may then define a unique dislocation velocity  $\mathbf{v} = \mathbf{v}^{\parallel} = \mathbf{v}^{\perp}$ , with

$$v_j = \frac{8\pi^2}{5(|\mathbf{b}|^2 + a^2|\mathbf{d}|^2)} \sum_{n=0}^4 \frac{J_{n,j}^D}{D_n} \Big|_{\mathbf{r}=\mathbf{0}} = \frac{1}{2} \sum_{n=0}^4 \frac{J_{n,j}^D}{D_n} \Big|_{\mathbf{r}=\mathbf{0}}, \quad (\text{S-57})$$

where we used that  $|\mathbf{b}|^2 + a^2|\mathbf{d}|^2 = 16\pi^2/5$ . By expressing the amplitudes in terms of their phase ( $\eta_n = |\eta_n|e^{i\theta_n}$ ) and computing both  $\mathbf{J}^D$  and  $D_n$  to the leading order we obtain

$$\frac{J_{n,j}^D}{D_n} \Big|_{\mathbf{r}=\mathbf{0}} = \frac{8A}{s_n} \epsilon_{jlk_n,l} k_{n,m} \partial_m \theta_n \Big|_{\mathbf{r}=\mathbf{0}}, \quad (\text{S-58})$$

where  $\theta_n$  is the amplitude phase. For QCs, using Eq. (S-35) to express the phases in terms of the displacements  $\mathbf{u}$  and  $\mathbf{w}$ , this becomes

$$\frac{J_{n,j}^D}{D_n} \Big|_{\mathbf{r}=\mathbf{0}} = \frac{8A}{s_n} \epsilon_{jlk_n,l} k_{n,m} (k_{n,o} \partial_m u_o + a q_{n,o} \partial_m w_o) \Big|_{\mathbf{r}=\mathbf{0}}, \quad (\text{S-59})$$

Then, we can rewrite Eq. (S-57) as:

$$\begin{aligned}
 v_j &= 4A\epsilon_{jl} \sum_{n=0}^4 \frac{1}{s_n} k_{n,l} k_{n,m} (k_{n,o} \partial_m u_o + a q_{n,o} \partial_m w_o) \Big|_{\mathbf{r}=\mathbf{0}} \\
 &= 4A\epsilon_{jl} \left[ \sigma_{lm}^{\parallel} \left( \sum_{n=0}^4 \frac{k_{n,m}}{s_n} \right) + a \sigma_{lm}^{\perp} \left( \sum_{n=0}^4 \frac{q_{n,m}}{s_n} \right) \right] \Big|_{\mathbf{r}=\mathbf{0}}.
 \end{aligned} \tag{S-60}$$

We can evaluate the sums

$$\begin{aligned}
 \sum_{n=0}^4 \frac{k_{n,m}}{s_n} &= \frac{5}{4\pi} b_m, \\
 \sum_{n=0}^4 \frac{q_{n,m}}{s_n} &= \frac{5a}{4\pi} d_m,
 \end{aligned} \tag{S-61}$$

substituting which into Eq. (S-60), and exploiting the linear strain-strain relations we get the expression for the velocity reported in the main text:

$$v_i = \frac{5A}{\pi} \epsilon_{ij} \left( \sigma_{jk}^{\parallel} b_k + a^2 \sigma_{jk}^{\perp} d_k \right). \tag{S-62}$$

---

\* [marco.salvalaglio@tu-dresden.de](mailto:marco.salvalaglio@tu-dresden.de)

- [S1] D. Levine, T. C. Lubensky, S. Ostlund, S. Ramaswamy, P. J. Steinhardt, and J. Toner, *Phys. Rev. Lett.* **54**, 1520 (1985).
- [S2] M. Salvalaglio and K. R. Elder, *Model. Simul. Mater. Sci. Eng.* **30**, 053001 (2022).
- [S3] J. E. S. Socolar and P. J. Steinhardt, *Phys. Rev. B* **34**, 617 (1986).
- [S4] P. J. Steinhardt, H.-C. Jeong, K. Saitoh, M. Tanaka, E. Abe, and A. Tsai, *Nature* **396**, 55 (1998).
- [S5] P. Hirvonen, V. Heinonen, H. Dong, Z. Fan, K. R. Elder, and T. Ala-Nissila, *Phys. Rev. B* **100**, 165412 (2019).
- [S6] V. Skogvoll, A. Skaugen, and L. Angheluta, *Phys. Rev. B* **103**, 224107 (2021).
- [S7] C. V. Achim, M. Schmiedeberg, and H. Löwen, *Phys. Rev. Lett.* **112**, 255501 (2014).
- [S8] N. Goldenfeld, B. P. Athreya, and J. A. Dantzig, *Phys. Rev. E* **72**, 020601(R) (2005).
- [S9] N. D. Mermin and S. M. Troian, *Phys. Rev. Lett.* **54**, 1524 (1985).
- [S10] R. Lifshitz and D. M. Petrich, *Phys. Rev. Lett.* **79**, 1261 (1997).
- [S11] D. Levine and P. J. Steinhardt, *Phys. Rev. Lett.* **53**, 2477 (1984).
- [S12] L. Benoit-Maréchal and M. Salvalaglio, *Model. Simul. Mater. Sci. Eng.* **32**, 055005 (2024).
- [S13] P. De and R. A. Pelcovits, *Phys. Rev. B* **35**, 8609 (1987).
- [S14] D.-h. Ding, W. Yang, C. Hu, and R. Wang, *Phys. Rev. B* **48**, 7003 (1993).
- [S15] M. Salvalaglio, A. Voigt, and K. R. Elder, *npj Comput. Mater.* **5**, 48 (2019).
- [S16] G. F. Mazenko, *Phys. Rev. Lett.* **78**, 401 (1997).
- [S17] A. Skaugen, L. Angheluta, and J. Viñals, *Phys. Rev. B* **97**, 054113 (2018).
- [S18] V. Skogvoll, L. Angheluta, A. Skaugen, M. Salvalaglio, and J. Viñals, *J. Mech. Phys. of Solids* **166**, 104932 (2022).
- [S19] V. Skogvoll, J. Rønning, M. Salvalaglio, and L. Angheluta, *npj Comput. Mater.* **9**, 122 (2023).